A short review of numerical cloud-resolving models

Françoise Guichard & Fleur Couvreux

Published online: 19 Sep 2017.

Submit your article to this journal

Article views: 909

View related articles

View Crossmark data

A short review of numerical cloud-resolving models

By FRANÇOISE GUICHARD* and FLEUR COUVREUX
CNRM, CNRS UMR 3589 and Météo-France, Toulouse, France

ABSTRACT

A cloud-resolving model (CRM) allows performing numerical simulations of convective clouds, such as shallow cumulus and stratocumulus, or storms and squall-lines with a resolution on the order of a few tens of metres to a few kilometres over a limited-area 4D (time and space) domain. The development of such models over the past decades is reviewed and their specific features are presented. The latter include a non-hydrostatic dynamic and parameterizations of sub-grid turbulence, microphysical and radiative processes. The capabilities of such models are discussed based on comparisons with observations and model-intercomparison studies. CRMs are used in a variety of ways, from the exploration of cloud phenomenology and process-understanding studies to the development of algorithms for satellite products, as well as to address climate issues and to develop convective and cloud parametrizations for large-scale weather and climate models. A few results illustrating this wide utilization are presented. The continuous increase of computer power induces rapid changes in modelling perspectives and therefore, influences the developments and applications of CRMs. This is discussed together with emerging scientific questions which will further benefit from CRM simulations.

Keywords: atmospheric convection, clouds, numerical modelling, convection-permitting simulation, large-eddy simulation, physical processes, parametrizations, turbulence, microphysics, radiative transfer

1. Introduction

Most people have, more than once in their life, observed the shallow cumulus clouds frequently arising from a clear sky on fair weather days, experienced heavily precipitating storms or complained about stratocumulus decks dimming sunshine. These are all common meteorological phenomena and they are associated with the development of atmospheric circulations whose space and time scales typically range from a few tens of metres to a few hundreds of kilometres and from a few minutes to several hours; these scales are traditionally referred to as micro- and mesoscale. These circulations are strongly coupled to moist thermodynamic and microphysical processes (formation and growth of liquid droplets and ice particles, melting of snow, evaporation of rain drops). In the 'dry' convective boundary layer, vertical motions develop in an asymmetric way (Schmidt and Schumann (1989). Cloud-circulations are characterized by an even stronger asymmetry between narrow, strong in-cloud vertical motions associated with latent heat release and wider, weaker fluctuations taking place in their clear-sky surroundings. As opposed to larger-scale atmospheric circulations, these transient motions are characterized by strong fluctuations of vertical velocity, in other words, the hydrostatic equilibrium breaks down at these finer scales where the convective dynamics

(which involves turbulent vertical motions, moist physics – including, condensation of water vapour, formation of precipitation, evaporation – and their mutual interactions) play a major role.

As a result, the modelling of these familiar but highly non-linear phenomena turns out to be particularly challenging in practice. Only limited insight can be gained from analytical approaches because of the very nature of the processes. Precious guidance is obtained from observations but observations alone are generally too limited to provide definite answers to the numerous questions raised by transient convective clouds. Indeed, the first detailed in-cloud aircraft data of the 60s and 70s already revealed a complex reality that departed in many ways from the hypotheses or concepts underlying the first simplified models of clouds. For instance, the formulation of mass exchanges between clouds and their surroundings was questioned by Warner (1970) – see also Malkus (1953). Several decades later, this topic is still the object of debate and active research (Siebesma and Holtslag, 1996; Jonker et al., 2008; Romps and Kuang, 2010; de Rooy et al., 2013).

Even, in the late 60s and later, it seems that fully parametrized models of cumulus clouds were considered by several researchers as a more fruitful avenue than the first attempts to simulate them numerically in a more explicit way (e.g. see the

---

*Corresponding author. e-mail: francoise.guichard@meteo.fr

1

comment of Simpson and Wiggert (1969) on the work of Ogu-ra (1963) and others, also Redelsperger pers. comm.). In the face of such pessimistic perceptions, the research carried out in the following 40 years nevertheless led to the development of several numerical models that explicitly simulate unsteady convective clouds, and these models are now widely used in the atmospheric and climate research community as will be seen below. They are often referred to by the two acronyms LES and CRM, for large-eddy simulation and cloud-resolving model (note that other acronyms found in the literature, such as CEM for cloud ensemble model, or CSRM for cloud system-resolving model refer to CRM as well).

Here, we present a short review of these types of models. It is not intended to be a detailed and exhaustive survey. Rather, its main objective is to provide important primary information to the growing number of researchers who work with, or come to use results from these types of models. The presentation starts with an overview of their main characteristics and strengths (Section 2) and continues with a brief history of their development since the 70s (Section 3). The formulation of these models is presented and discussed in Section 4, with details about their parametrizations and commonly used initial and boundary conditions. Finally, a few examples of their performance and utilization are given in Section 5.

2. Main characteristics of cloud-resolving models

2.1. A model resolving convective moist phenomena of transient nature

By design, a LES, or similarly a CRM, is a numerical model whose grid-spacing is fine enough to allow explicit simulations of individual clouds, throughout their whole life cycle or over part of it. In atmospheric sciences, the distinction between LES and CRM can be viewed as largely historical. It has its roots in the parallel development of two types of explicit cloud models dedicated to the studies of smaller and shorter-lived shallow cumulus vs. wider and longer-lasting deep convective clouds. With respect to turbulent motions, the theoretical foundations of LES were more clearly defined from the start, as LES were designed to resolve turbulent motions down to the inertial subrange (Pope, 2000; Bryan et al., 2003). Indeed, LES were inherited from computational fluid dynamics and first used for atmospheric turbulence in the 60s (Smagorinsky, 1963; Deardorff, 1970). A LES is a self-consistent technique, which applies a high-pass filter to the Navier–Stokes equations in order to avoid the computational cost of resolving all the scales of motion and makes use of models (or parametrizations) to represent sub-grid scale motions; it is very well suited for the simulation of turbulent motions in atmospheric convective boundary layers (Stevens and Lenschow, 2001; Moeng and

Sullivan, 2002). By contrast, the motivation underlying the development of CRM was, from the start, to better understand convective cloud-related transient motions involving water phase changes in the atmosphere with models that explicitly resolved deep convective motion. It is also worth noting that the early developments of LES and CRM occurred at about the same time, but without much interactions between the two scientific communities at first (Wyngaard, 2004).

However, beyond differences in their formulation of sub-grid processes (including turbulent motions, but also microphysical and radiative processes), the underlying equations of CRMs and LES are very similar, and the distinction between the two now often refers to the utilization of finer vs. coarser grids in numerical simulations. Indeed, the spatial resolution of a simulation is also intuitively determined by the object under study. It is typically around 1 km in CRM simulations of deep clouds and 100 m in LES simulations of shallow cumulus and stratocumulus. Considerations of the same type dictate the choices for domain size and duration of a simulation. Thus, one to a few hours of simulation performed over a 10 km-wide and 5-km high domain is typically well suited to model a few coexisting shallow cumulus clouds and to sample their individual life cycles. A 100-km wide 20-km high domain and several hours of simulation become necessary when focussing on deep convective cloud cells reaching the top of the troposphere (these numbers are more indicative of lower space and time limits). Nowadays, LES and CRM are often used to perform simulations over much wider domains and longer durations. Note also that in the past, many LES incorporated parametrizations of the microphysics that are traditionally referred to as 'warm'. These parametrizations discard processes involving the solid phase of water and are well suited to study 'warm' shallow cumulus clouds in the tropics (as their tops stay well below the isothermal 0 °C). On the other hand, the importance of ice-phase microphysics to deep convection, which typically extends far above the 0 °C isothermal, was identified quite soon, and sophisticated parametrizations of ice-phase processes were introduced in some CRMs in the early 80s (Lin et al., 1983).

2.2. A numerical tool to further process understanding and to explore scientific questions

Figure 1a displays a schematic view of a population of tropical clouds over ocean inferred from observations (Houze et al., 1980; Houze and Betts, 1981) and Fig. 1b a three-dimensional (3D) snapshot of an ensemble of clouds independently simulated with a CRM (Guichard et al., 1997). Figure 1b was not at all drawn to mimic Fig. 1a, still both figures share a number of similarities such as the growing deep convective cells ahead of the system and the thick anvil-type cloud at its rear. A first major interest of the simulation is to provide space- and time-varying (four-dimensional) fields of both temperature, water vapour and cloud and rain water, horizontal and vertical wind fields together with details of the numerous operative processes.
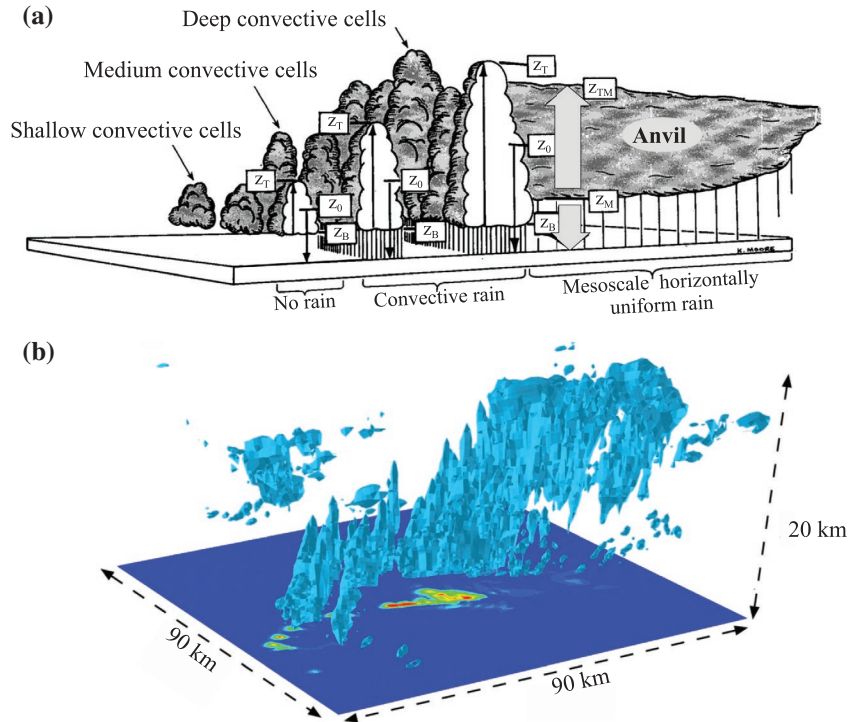
Fig. 1. (a) Schematic of a population of clouds over a tropical ocean; thin (thick) arrows represent convective (stratiform) updraught and downdraught, while heavy convective (lighter stratiform) rain is indicated by narrow (wider) hatchings – adapted from Houze et al. (1980), ©Copyright 1980 American Meteorological Society (AMS), see also Houze and Betts (1981). (b) Three-dimensional view of a cloud field simulated by a CRM – adapted from Guichard (1995), see also Guichard et al. (1997).

Such a comprehensive set of information on transient convective phenomena cannot be obtained from observations alone. Furthermore, a number of diagnostics can be derived from CRM simulations, via the analysis of budget equations, of the space and time patterns and distributions of variables, or the use of tracers. Figure 2 illustrates the typical structure of thermodynamic budgets in a convective atmosphere over ocean, where the vertical structures of heating and drying are not solely explained by the microphysics, but also by convective motions, which account for substantial transport of water vapour from the lower to the upper troposphere. Sensitivity tests can be performed too. For instance, one may explore the importance of the humidity field on the structure, strength and vertical extent of convection by comparing simulations using different initial water vapour fields, or test the impact of evaporative processes on the strength of convection by either allowing or suppressing them. Indeed, numerous fundamental questions remain about convective clouds. The factors accounting for their spatial structure and for their spectrum of size and spacing are not all well understood nor possibly fully identified. Still, well-defined recurrent mesoscale geometric patterns are observed and they are often quite spectacular. They take the form of fair-weather scattered cumulus clouds which materialize convective open
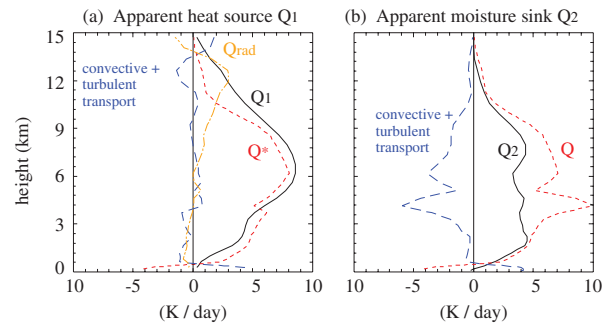

Fig. 2. Vertical structure of the convective processes operating in the budget of temperature (a) and water vapour (b) within an atmosphere experiencing deep convection over a tropical ocean. The solid black lines corresponds to the apparent heat source and moisture sink (Q_1, Q_2) that are parametrized in large-scale models; the red dotted, blue dashed and orange dashed-dotted lines indicate, respectively the total latent heat release due to microphysical processes (Q^*, Q), the impact of turbulent and convective transport, and divergence of radiative fluxes (Qrad). (Results from a CRM simulation presented in Guichard et al. (2000), the slots show seven-day mean profiles over an area 256 km wide.)

cells having their roots in the boundary layer, or appear as lines of cloud streets or lines of 'pearls on a string' (Kuettner, 1971). In contrast to scattered cumulus, stratocumulus fields often

display closed-cell structures (Atkinson and Zhang, 1996; Wood and Hartmann, 2006). Deep convection sometimes aggregates into wider multicellular structures, an archetypical example being the squall-line with its dense line of deep convective cells ahead of a wide and thick stratiform anvil. LES and CRM are powerful tools to address this wide range of fundamental scientific questions within a tightly controlled framework, as illustrated in Section 4.

The strength of such simulations is to provide an *explicit* representation of the clouds and associated motions arising at scales larger than the smallest resolved motions (namely, a few tens for a LES to a few hundreds of metres at best for a CRM). One must not mistake these simulations for reality though, nor substitute them for observations. Indeed, we know from aircraft *in situ* data that turbulent fluctuations are still observed within clouds at scales smaller than 100 m (e.g. Warner, 1970). Sub-grid-scale motions, together with microphysical, and sometimes radiative processes, are taken into account in CRMs, albeit implicitly, via parametrizations that are presented in Section 3. Observations are also of major importance. First, they allow us to characterize atmospheric convection and to identify relevant scientific questions. They have inspired numerous modelling studies, perhaps even more so now than 30 years ago, due to the increase in number and type of observational studies. From a more practical perspective, they provide major guidance to design simulations, notably for the choice of initial and boundary conditions.[1] Observations also greatly help to assess the relevance of the simulations, and to evaluate and improve parametrizations. Conversely, CRM simulations provide a precious tool to interpret observations which are often sparse and incomplete with regards to the transient nature of convective cloud-related processes and to the questions at hand. Those models can thus be seen as a bridge between observations and parametrized models.

Finally, another growing type of utilization of CRM simulations is dedicated to the improvement or development of new parametrizations of convective processes. In short, results from CRMs are taken into account and used for guidance. Provided that enough care is taken in comparing explicit and parametrized simulations, and importantly, that the focus remains on robust features of the explicit simulations, valuable inferences can be obtained. The CRM is then used as a *numerical laboratory* to further the understanding of interactions among processes and to design more physically-based formulations for parametrized models. The development of single-column model (SCM) versions of large-scale weather or climate models integrating the same set of parametrizations greatly helped in the success of this approach, because the comparison of the results obtained with single-column and cloud-resolving models becomes much more direct (Randall et al., 1996). This is discussed in more detail in Section 5.3.

2.3. Where CRMs stand with respect to emerging high-resolution modelling systems

Now that CRM simulations of squall-lines can be performed with a LES-type resolution (of about 100 m, Bryan et al., 2003), the distinction between these two types of models tends to become blurred, even if LES of shallow convection are performed with ever finer resolution (e.g. Matheou et al., 2011).

The situation is even more confusing when considering the evolution of larger-scale models. Indeed, until very recently, the resolution of numerical weather forecast models (several tens of km) was too coarse for them to explicitly resolve any convective processes; these processes were only implicitly represented with parametrizations. However, nowadays, several numerical weather models employ a horizontal grid size of a few km and, accordingly, they have modified their equations, switching to a non-hydrostatic dynamic of the atmosphere (Seity et al., 2011 for instance). One can also think of recent simulations performed over domains several tens of degrees wide with horizontal grid sizes finer than 5 km, often referred to as 'convection-permitting simulations' (e.g. Marsham et al., 2013). Some global simulations have even been performed with such a configuration (Tomita et al., 2005; Satoh et al., 2008; Miyakawa et al., 2014). Note also the existence of conceptually more complex types of GCMs: these are embedding a CRM within each of their atmospheric columns (Khairoutdinov et al., 2005), an approach advocated by Randall et al. (2003) which uses the so-called super-parametrization framework initially imagined by Grabowski (2001). More recently, Grabowski (2016) even proposed to use 3D LES (instead of coarser-grid 2D CRM) in such GCMs.

The emerging overlap between CRMs and GCMs indicates that the 'traditional' view of what a CRM stands for would benefit from some clarifications. Alternatively, in the future, a CRM could well be defined as a model within which the fine-scale non-hydrostatic motions and their interactions with physical processes (microphysics, radiation) are explicitly taken into account, regardless of the model being a narrow limited-area model dedicated to mesoscale studies or a global model allowing in-depth studies of the interactions and couplings between convective processes and the larger-scale circulations.

The examples above indicate that increase of computation power opens the door to new types of approaches for studying moist convective processes. However, even if this power was to increase to the point where all GCMs were able to afford a 1-km grid in the close future, limited-area 'traditional' CRMs would certainly continue to be useful for many reasons. First, it remains a well-suited tool to study processes and mechanisms within simplified frameworks, for academic[2] purposes and also to interpret more complex models. More fundamentally, numerous issues still need attention as do further developments in current CRMs. This notably includes (i) the parametrization of boundary-layer turbulent motions (with a 1 km resolution,

these motions are partly resolved, partly parametrized, and their representation in CRMs is not yet satisfying – e.g. Honnert et al., 2011), (ii) radiative processes (for instance, in most CRMs, radiative processes are treated independently within each individual column without any interactions) and (iii) last but not least microphysical processes. Furthermore, couplings of LES and CRMs with land and ocean surface models also require new careful developments. This discussion will be developed later, but first, we go back to recall the pioneering days of explicit simulations of cumulus clouds.

3. Back to the origins

In meteorology, the acronyms LES and CRM appeared, respectively in the 80s and 90s, but the development of these types of models can be traced back to the 60s and 70s. This process is briefly recalled below.

3.1. First LES of shallow cumulus clouds and stratocumulus decks

The first large-eddy simulation of trade-wind cumulus clouds was achieved by Sommeria (1976), and rested upon extending a model first developed by Deardorff (1972) for the simulation of the 'dry' (i.e. cloud-free) convective boundary layer. In order to simulate cumulus clouds, Sommeria (1976) introduced a parametrization of condensation and evaporation processes together with an additional prognostic equation for the cloud-water mixing ratio, with liquid water assumed to take the form of cloud droplets in suspension that are advected with the flow. With this model, he was able to simulate shallow cumulus clouds with a horizontal resolution of 50 m over a 2 km-wide domain for five hours (Fig. 3). Albeit simple, the setup of the simulation was not unrealistic. Initial conditions were

cloud-free, with thermodynamic and dynamic profiles derived from a radio-sounding, and a given value of SST was prescribed at the surface. The model also took into account longwave radiation and a prescribed larger-scale flow. With these settings, a statistical steady-state was reached after an hour of simulation. This pioneer study also showed that heat and moisture fluxes were highly variable in time and space in the cloud layer (in relation to condensation and evaporation processes) and even evidenced the presence of subsidence at the edge of individual clouds. During this same decade, Asa and Nakamura (1978) also developed a two-dimensional (2D) LES that provided qualitatively similar results.

Shortly after, a parametrization of sub-grid condensation was introduced in the 'Sommeria's model' by Sommeria and Deardorff (1977). They assessed that even with a relatively fine mesh on the order of 50 m, the assumption that such a mesh should be entirely saturated or entirely unsaturated was crude, a finding further corroborated by observations (Sommeria and LeMone, 1978). This sub-grid scheme assumed Gaussian distributions for the liquid potential temperature and the total water mixing ratio in the mesh. In retrospect, this appears as a too simple assumption. Indeed, the distributions of dynamic and thermodynamic variables can be highly skewed in a convective atmosphere (Weckwerth et al., 1996; Couvreux et al., 2007; Sullivan and Patton, 2011), and they are profoundly modified by moist convection (Siebesma and Holtslag, 1996; Zhu et al., 2010). Work is still ongoing today to improve the representation of small-scale distributions of thermodynamic variables in cloud fields. Bougeault (1981) highlighted the interest of a skewed distribution with a long flat-tail related to shallow convection, and since then numerous other joint probability distribution functions of vertical velocity, liquid potential temperature and total water vapour mixing ratio have been proposed (Larson et al., 2002 among others). Note that because the grid size is
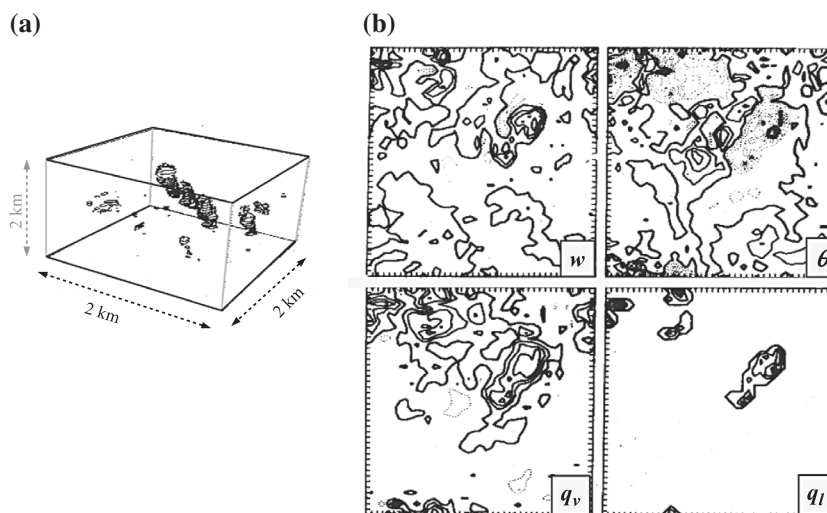

Fig. 3. Illustration of one of the first LES of shallow cumulus clouds: (a) 3D view of the cumulus simulation after 4 h of simulation. The domain is a $2 \times 2 \times 2$ km^3 cube and the grid size is 50 m in all three directions, (b) horizontal cross-sections at 775 m of the vertical velocity (w), potential temperature (θ), specific humidity (q_v) and liquid mixing ratio (q_l), with interval between isolines of, respectively, 0.61 m s^{-1}, 0.92 K, 0.42 g kg^{-1} and 0.091 g kg^{-1} – these cross-sections highlight the strong correlations among those variables – adapted from Sommeria (1976), ©Copyright 1976 AMS.

coarser in CRMs than in LES, the contribution of the sub-grid cloud scheme may typically be more important in a CRM than in a LES.

Improvements in the parametrization of the sub-grid turbulence were further carried out by Redelsperger and Sommeria (1981) with (i) the introduction of a prognostic equation for the turbulent kinetic energy (TKE) and the (ii) use of thermodynamic variables, approximately conserved when water changes phase, and therefore more suited for the formulation of the interactions between turbulent motions and moist thermodynamics. At about the same time, Deardorff (1980) simulated a stratocumulus-capped mixed layer over land with this model, albeit with modifications at the lower boundary in order to account for the distinct balance of turbulent fluxes over a land surface. In this study, he explored in particular the role of cloud-top radiative cooling with a suite of sensitivity tests, including dry and 'smoke-cloud'[3] topped boundary layers, as well as stratocumulus decks that were not interacting with radiative processes. They notably concluded that future simulations should use a finer vertical spacing than the 50 m used in order to properly simulate the processes occurring near the thermodynamic inversion at the cloud top and to avoid truncation errors.

Later, Redelsperger and Sommeria (1986) introduced a formulation of precipitation processes (following Kessler, 1969), which made use of a new prognostic equation for a rain water mixing ratio variable (the latter departs from cloud water in that rain droplets fall with respect to the fluid they are embedded in). In a similar spirit, Krueger (1988) developed a two-dimensional precipitating cloud model, applying great care to the formulation of turbulence (in this case with the first implementation of a third-order scheme in such models). According to their grid size (~1 km), the simulations presented in Redelsperger and Sommeria (1986) and Krueger (1988) can be viewed as CRM-type simulations. However, both models were either developed from, or inspired by LES of clouds, with particular attention paid to the representation of sub-grid-scale turbulence, and this tight connection differentiates them from other CRMs developed at that time.

In the following decades, various developments improved these models. On the process side, motivated by the need for a better representation of drizzle-related processes, Kogan et al. (1995) introduced a representation of the microphysical processes based on an explicit formulation of a droplet size distribution function (the drops are distributed among different sizes and drops of each size are subjected to advection by wind, condensation, sedimentation). New simulation set-ups were also designed for studying the transition from the stratocumulus to the trade-wind cumulus regime. Krueger et al. (1995) and Wyant et al. (1997) simulated cloudy air motions in a Lagrangian-type domain, which moved with the mean boundary-layer wind in a dynamic larger-scale environment (where sea surface temperature, free tropospheric temperature, mixing ratio and subsidence evolved). At the same time, a framework was established by Grabowski et al. (1996) to formulate time-varying large-scale advection in CRMs with periodic lateral conditions. This opened the way to simulations that could be driven by observationally-based large-scale advection, and allowed exploration of the influence of day-to-day changes in the large-scale environment on convective activity (e.g. Wu et al., 1998). Furthermore, this approach proved to be valuable for observationally-based model evaluation as well (e.g. Xu and Randall, 1996).

In terms of numerics, LES greatly benefited from numerical techniques using Fourier transform that were developed in computational fluid dynamics for periodic flows (e.g. Orszag, 1971; Moeng, 1984; Schumann and Sweet, 1988). More recently, Raasch and Schröter (2001) presented the first LES run on a massively parallel system with distributed memory. This opened the possibility of longer simulations over much larger domains, which allows tacking new scientific questions, such as the causes behind the mesoscale structures of convective clouds and the transition of regimes.

In the last 30 years, LES of clouds have been widely used, with either academic, idealized or more realistic set-ups, and some examples of results obtained from those simulations will be presented in Section 5.

3.2.   From CRM modelling of convective cells to LES of squall-lines

In the 70s, the novelty of the first ancestors of the models now referred to as CRMs were lying in their formulation of the non-hydrostatic dynamics. This allowed an explicit treatment of the couplings arising between convective-scale motions, thermodynamic and microphysical processes. As for LES, in practice this also meant introducing and solving new prognostic equations for vertical velocity and cloud water, but in addition also for rain water. In retrospect, several aspects of these models and of the simulations carried out at that time may appear rudimentary. One must keep in mind that the computing capabilities were considerably less than today though. Even more critical, it was necessary to first solve numerous theoretical and numerical difficulties, from the definition and discretization of well-suited, tractable equations, including the formulation of appropriate initial and boundary conditions to the introduction of parametrizations for microphysical processes, again with the constraint of limited computing power. In fact, by demonstrating the relevance and potential of this numerical approach, these pioneering works paved the way for the subsequent development and further utilization of this type of modelling to study convective clouds.

For instance, Miller and Pearce (1974) developed one of the first three-dimensional non-hydrostatic models of deep precipitating convection. Such a model proved to be able to simulate the development of a single deep convective cell within a 15 km wide domain extending up to the tropopause, from a local per-

turbation added in the lower levels of an otherwise horizontally homogeneous initial atmospheric state. Note that, by design, this small-size domain precluded the simulation of the interactions arising between deep convection and the larger-scale circulations. Still, the simulation highlighted the strong couplings arising at small spatio-temporal scales between convective motions and microphysical processes, the importance of water loading to the cloud dynamics, and of rainfall evaporation to downdraught formations (these issues are discussed in more details in Section 4).

In the following decade, these models benefited from numerous numerical and physical improvements (e.g. Klemp and Wilhelmson, 1978), and by the early 80s, they started to be used to study the dynamics of deep convective clouds, the links between their morphology and the wind field, the role of convectively generated outflows on subsequent convective developments, or the splitting of convective storms and generation of new cells (Wilhelmson and Klemp, 1981).

It is worth noticing that several cloud models were built in the 70s and 80s across the world. The distinct underlying objectives leading to their developments readily translated into some differences in their numerical schemes, their formulations of initial and boundary conditions, and into various degrees of sophistication in their physical parametrizations. In the 80s, these models were further used to study the morphology and life cycle of individual storms, or to explore the mechanisms at play in wider mature squall-lines, in particular, the drivers of their self-sustained nature, with numerical simulations lasting a few hours.

The promising capabilities of this new modelling approach also motivated other uses which led to additional developments. For instance, some models or model configurations were specifically designed for the purpose of studying the main features and sensitivities of not a single storm but ensembles of deep clouds evolving within, and interacting with, a wider larger-scale environment (Tao and Soong, 1986; Krueger, 1988; Gregory and Miller, 1989; Xu et al., 1992; Held et al., 1993; Tompkins and Craig, 1998). Such a configuration allowed addressing the simulated convective atmosphere's sensitivity to SST, large-scale wind fields and microphysical processes with a new, much less parametrized type of model than those previously used in the past, such as the one-dimensional (1D) single-column approach pioneered by Manabe and Wetherald (1967). For these type of studies and others, the need of wide-enough environments and long duration runs led to the design and frequent use of two-dimensional simulations in the 80s and 90s. This choice may appear surprising because such a framework fails to reproduce the inherently three-dimensional structures of convective processes. Still, it provided an explicit treatment of the tight couplings arising between convective motions, microphysical and radiative processes. 2D CRMs present a number of obvious limitations such as a tendency to artificially
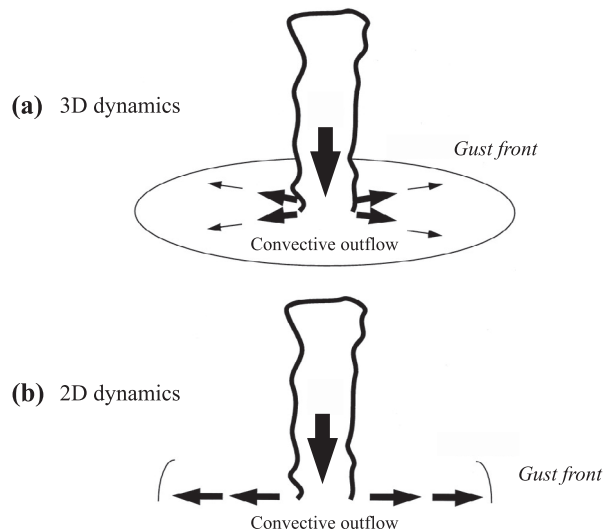

Fig. 4. Schematic of expected differences in surface winds between a 3D (a) and a 2D (b) simulation. The arrows indicate the surface winds resulting from downdraught spreading at the surface as a cold pool, with thicker arrows representing higher velocities – adapted from Tompkins (2000), © Copyright 2000 AMS.

prevent the weakening of low-level cold pools (Fig. 4) and to favour the mesoscale aggregation of convection (Grabowski et al., 1998; Tompkins, 2000; Redelsperger et al., 2000a). However, its use proved to be fruitful in advancing on some issues that were, in the end, not very affected by these limitations, or at least less so than by other more critical choices such as details of the microphysical parametrizations in multi-day CRM simulations (Guichard et al., 2000). Nevertheless, with continuously increasing computing power, performing three-dimensional simulations has become more affordable, and 3D simulations of mesoscale convective systems (MCS) are now common.

4. Formulation of the model

4.1. *Non-hydrostatic dynamics, prognostic clouds and other chief features*

In terms of dynamics, both LES and CRM share an important feature, they are both non-hydrostatic types of models. The *non* in *non-hydrostatic* reminds that historically, the system of equations adopted by meteorological models made use of the hydrostatic approximation which assumes a balance between the force of gravity and the pressure force. In that case, the vertical acceleration vanishes and the vertical velocity, *w,* becomes a diagnostic variable (see for instance Trapp, 2013).

However, the fluctuations of *w*, even if relatively small compared to the force of gravity and pressure force cannot be

neglected at scales less than 10 km. From physical considerations as well, fluctuations of vertical velocity, which correspond to departure from a hydrostatic state, are a major expression of atmospheric convective motions (Yau, 1979). Besides, theoretical considerations imply that the strengthening of vertical motions arising at smaller scales is less than would occur if the dynamics was purely hydrostatic (in that case, the vertical velocity increase would be proportional to the inverse of the horizontal scale, Weisman et al., 1997). Therefore, both LES and CRMs incorporate a prognostic equation for the vertical velocity.

Originally, a large-eddy simulation refers to a numerical model based on the resolution of the Navier–Stokes equations which explicitly simulates turbulent motions. The same definition can be retained for LES and CRM of moist and cloudy atmospheric flows, with turbulence including convective motions arising on scales below a few to several tens of kilometres. These equations are spatially and temporally filtered and the smaller-scale turbulent motions are represented via parametrizations (see Mason, 1989 for details). In LES, the filter width generally coincides with the grid size. LES differs from a direct numerical simulation (DNS), as the latter resolves all scales of motion (for the atmosphere, it means a horizontal resolution of a few cm). Accordingly, DNS are also more expensive and currently hardly tractable to simulate atmospheric flows in the same way as currently possible with LES (DNS are nevertheless very informative for specific focused scopes such as the exploration of thin stratocumulus cloud tops and cumulus cloud edges; e.g. Mellado et al., 2009).

In LES and CRMs, it is generally assumed that pressure fluctuations balance rapidly and are negligible in comparison to density or temperature fluctuations, this is the anelastic approximation (Ogura and Phillips, 1962). Its main interest is to allow the filtering of high-velocity waves, sound waves in particular; the pressure is then obtained from an elliptic equation. The main advantage of an anelastic formulation is thus to allow for longer time steps as the high speed of sound waves requires the use of very small time steps in finite-difference schemes due to the CFL (Courant–Friedrichs–Lewy) criterion (which corresponds to a necessary condition for the convergence of computations done with this type of numerical scheme). In some cases, density fluctuations can further be considered as negligible in the continuity equation; in other words, the air is assumed incompressible (or non-divergent); this is the Boussinesq approximation. It is not valid for deep convection which develops within much deeper air layers whose density decreases at lower pressure heights, but has been often used in LES of shallow flows, for instance, in simulations of turbulent motions confined to the first kilometres of the atmosphere above the surface.

There are some limitations to the anelastic approximation of Ogura and Phillips (1962), in particular with respect to the conservation of mass and energy, and a few dedicated studies attempt to improve its original formulation in current models

(Durran, 1989; Bannon, 1996; Arakawa and Konor, 2009). Note however, that a few CRMs have been developed from the outset without this approximation (e.g. Klemp and Wilhelmson, 1978; Romps, 2008), but in that case specific numerical methods had to be developed.

The choice and number of prognostic variables also vary from one model to the other, but a minimal set, well suited to simulated non-precipitating shallow cumulus clouds, typically includes prognostic equations for the three components of the wind (u, v, w), for one temperature variable (e. g. either just the temperature, the potential temperature or the liquid water potential temperature) and for two water variables (either specific humidity q_v and cloud water q_c, or water vapour and cloud mixing ratios r_v and r_c; in some models, total water is considered instead of water vapour). The number of 'water' variables is directly related to the microphysical scheme as discussed in Section 4.3.

Here, we present an example of one possible choice of basic equations for use in a CRM. It is important to realize that such a choice is not unique. For instance in this example, the anelastic assumption for density ρ is used (meaning ρ appears only as a function of height, noted ρ_r). z is used as the vertical coordinate, and the variables retained to formulate the prognostic equations of momentum, heat and water conservation are, respectively, the three components of the velocity (u, v, w), the potential temperature θ, the water vapour mixing ratio r_v, and the mixing ratio of each hydrometeor species r_x (e.g. liquid droplets, rain drops, ice, snow, graupels). The set of equations comprises:

- *The equation of state* $T/\theta = \left(\frac{P}{P_o}\right)^{\frac{R_d}{C_p}}$

where P is the pressure and T the temperature. P_o is a reference pressure, R_d is the universal gas constant for dry air and C_p is the specific heat coefficient.

- *The continuity equation* (mass conservation)

$$\rho_r \frac{\partial \bar{u}_j}{\partial x_j} + \bar{w}\, \frac{\partial \rho_r}{\partial z} = 0$$

- *The dynamic equation* (momentum conservation)

$$\begin{aligned}
\frac{\partial \bar{u}_i}{\partial t} \;=\; &-\; \frac{1}{\rho_r} \frac{\partial\left(\rho_r \overline{u_i u_j}\right)}{\partial x_j} \;-\; \frac{1}{\rho_r} \frac{\partial P}{\partial x_i} \\
&+\; \frac{g}{\theta_r}\left(\overline{\theta_{vl}} - \theta_r\right)\delta_{i,3} \;-\; \frac{1}{\rho_r} \frac{\partial\left(\rho_r \overline{u_i' u_j'}\right)}{\partial x_j} \\
&-\; 2\,\varepsilon_{i,j,k}\Omega_j\,\overline{u_k}
\end{aligned}$$

- *The thermodynamic equation* (heat conservation)

$$\begin{aligned}
\frac{\partial \bar{\theta}}{\partial t} \;=\; &-\; \frac{1}{\rho_r} \frac{\partial\left(\rho_r\, \overline{u_j \theta}\right)}{\partial x_j} \;-\; \frac{1}{\rho_r} \frac{\partial\left(\rho_r\, \overline{u_j' \theta'}\right)}{\partial x_j} \\
&+\; Q_{Rad} \;+\; Q_{m\Phi} \;+\; \left(\frac{\partial \bar{\theta}}{\partial t}\right)_{LS}
\end{aligned}$$

- *The prognostic equations of water vapour or hydrometeor species* (conservation of water)

$$\frac{\partial \overline{r_x}}{\partial t} = -\frac{1}{\rho_r}\frac{\partial\left(\rho_r \overline{u_j r_x}\right)}{\partial x_j} - \frac{1}{\rho_r}\frac{\partial\left(\rho_r \overline{u_j' r_x'}\right)}{\partial x_j}$$
$$+ S_x + \left(\frac{\partial \overline{r_x}}{\partial t}\right)_{LS}$$

Here, any variable α is expressed as $\alpha = \overline{\alpha} + \alpha'$, where $\overline{\alpha}$ corresponds to the mean value of α on the grid mesh and α' to its sub-grid fluctuation, and $\overline{u_j' \alpha'}$ is the turbulent flux of α.

Ω_j is the *j*th component of the earth's angular velocity and *g* the gravitational acceleration; θ_r is a reference potential temperature.

Q_{rad} is the radiative heating rate and $Q_{m\Phi}$ the heating rate associated with the microphysical processes (condensation, evaporation, precipitation, freezing), while S_x is the sum of the microphysical processes affecting r_x. The last term, indexed as *LS*, corresponds to the large-scale advection (see Section 4.5).

The virtual potential temperature, which is used in the buoyancy term of the momentum equation is expressed as $\theta_{vl} = \theta\left(1 + 0.61 q_v - q_t\right)$.

Other examples of sets of equations, presented in more detail, can be found in the literature, for instance in Lafore et al. (1998), Romps (2008), or Heus et al. (2010) among others.

Note that the formulation of the anelastic constraint leads to an elliptic pressure equation obtained from a combination of the continuity and momentum equations. This equation must be solved with accuracy, which is a non-trivial problem – see for instance, the numerical solutions adopted by Lafore et al. (1998) and reference therein, as well as the pressure solver of Maronga et al. (2015) for a LES using the Boussinesq approximation.

Several important numerical choices also have to be made in the design of a LES or a CRM. We only briefly discuss this issue below, but detailed information on the numerics of LES and CRM can be found in the textbooks of Sagaut (2006), Warner (2010), Wyngaard (2010), Cotton et al. (2010), Pielke Sr (2013).

In atmospheric sciences, most LES and CRM use finite-difference or pseudo-spectral methods for discretizing the set of equations in space and time. A commonly used vertical coordinate is the geometric height above the surface, but a 'terrain-following coordinate' is sometimes preferred (Gal-Chen and Sommerville, 1975; Schär et al., 2002 or Klemp, 2011). The size of the grid mesh is generally regular on the horizontal, with $\Delta x = \Delta y$. However, note that while the spatial grid in LES is often close to isotropy ($\Delta x = \Delta y \sim \Delta z \sim$ 50-100 m), it is generally stretched vertically in CRMs. More precisely, the discretization is much finer in the lower levels (less than 100 m) than above (a few hundred metres) for $\Delta x = \Delta y \sim$ 1 km. Thus, CRM grids are often highly anisotropic: this allows for a better resolution of the sub-cloud layer without increasing too much the computational cost. In LES and CRM, staggered grids are frequently used for the discretization of the set of equations, i.e.

different variables are defined at different points. For instance, with the widely used Arakawa staggered C-grid (Mesinger and Arakawa, 1976), scalar variables (e.g. θ, r_v) are defined at the centre of the ($\Delta x, \Delta y, \Delta z$) volumes and wind components at the edges of these volumes. The primary interest of the staggered grid, compared to a non-staggered grid, is that it increases the effective resolution of the model by decreasing the distance over which finite differences are computed. It also allows to filter out some computational modes.

The discretization of the set of equations on the numerical grid notably involves the choice of advection and time-stepping schemes. Various schemes are found in models, from simple to complex, centred or not, implicit or explicit, more or less diffusive and, finally, more or less conservative and accurate. Spatial gradients can be quite sharp in CRM simulations, notably at cloud edges. These concern momentum, but also scalars for which monotonic and positive definite schemes (e.g. Smolarkiewicz and Grabowski, 1990, Baba and Takahashi, 2013) are better suited (a positive definite scheme takes into account the fact that scalar variables have physical bounds; e.g. water vapour mixing ratio or turbulent kinetic energy values have positive values). High-order advection schemes typically insure a better accuracy, prevent spurious numerical oscillations around sharp gradients and increase the effective resolution. The effective resolution is sensitive to the implicit diffusion operated by the advection scheme. For instance, it can become coarser with a semi-implicit semi-Lagrangian scheme compared to an explicit scheme (e.g. Ricard et al., (2013). Explicit temporal integration schemes now often use splitting methods to improve computational efficiency, based on high-order Runge–Kutta methods (i.e. Wicker and Skamarock, 2002).

Even if one is not directly concerned with those numerical aspects of a model, it can still be necessary to precisely know the details of its grid, conserved variables, and advection schemes, for instance an off-line computation of fluxes or advection terms (i.e. afterwards, from the resolved variables of the model) will be less accurate if one uses another discretization that the one used in the model. Similarly, all CRM make some assumptions about the thermodynamics, i.e. they use simplified formulations of the thermodynamical equations and variables. Thus, when thermodynamical variables are consistently defined with those simplifications, they are expected to be better conserved (in the simulation) than when they are defined with more accurate formulations.

There are other numerical aspects to take into account, such as the ordering of the different computations required for each simulated process (where physical distinctions between slow vs. fast processes can help designing rules), or the formulation of the saturation adjustment (e.g. Tao et al., 1989).

Finally, it is worth noting that the recent study of Kurowski et al. (2014) suggest that in practice, the simulation of moist convection with a CRM is more sensitive to the numerics discussed above (e.g. advection schemes, grid size) and to

physical parametrizations (e.g. turbulence, microphysics) discussed below than to the choice of a compressible or anelastic atmosphere.

4.2. *Parametrizations of sub-grid-scale motions*

LES were initially designed to provide a statistical view of turbulent motions and it was assumed that sub-grid-scale turbulence is mainly isotropic and confined to the inertial range, whereas the larger eddies are resolved and depend on the environment. Most of the time, sub-grid-scale turbulent motions are taken into account by parametrizations based on local arguments with turbulent fluxes in the three directions expressed as a function of local gradients, i.e.:

$$\overline{u_i \alpha} = - K \frac{\partial \bar{\alpha}}{\partial x_i}$$

where K is a so-called eddy-diffusivity coefficient. However, the assumptions underlying such formulations typically break down close to the surface and in stable layers of the atmosphere where turbulent eddies become smaller and much less isotropic. Those schemes are referred to as eddy-viscosity sub-grid-scale models, and there are mainly two different schemes in use in current LES and CRM. The first one, initially developed by Lilly (1962) and Smagorinsky (1963) assumes that the buoyancy and shear productions of TKE balance the molecular dissipation. This leads to eddy diffusivities being proportional to local velocity and temperature gradients and function of a Richardson number (note that the constant of proportionality varies significantly from one model to the other) or expressed as a function of a Richardson number. The second, more sophisticated scheme (Lilly, 1967; Deardorff, 1980), introduces TKE in the formulation of eddy diffusivities, and involves the resolution of a prognostic equation for TKE. Both schemes incorporate a length scale which is often identified with the grid size except in stable layers, where it is reduced to avoid excessive turbulent mixing (e.g. Deardorff, 1980).

Alternative approaches and improvements to these schemes have been proposed. Notably, Germano et al. (1991) introduced a new dynamic sub-grid-scale modelling approach where the unknown coefficients introduced in the Smagorinsky-type formulation are computed dynamically, at every time and for each position in the flow instead of being given constant values. There are a few examples of application of this approach in LES of the atmospheric boundary layer (e.g. Basu and Porte-Agel, 2006; Vinkovic et al., 2006). Another approach was proposed by Misra and Pullin (1997) who represent sub-grid turbulence as stretched-vortical structures (Lungren vortices) whose orientations depends on the resolved flow. Recently, Chung and Matheou (2014) implemented such a sub-grid scheme in a LES of shallow convective clouds and showed that the results were close to those previously obtained with LES, and in addition, they were only weakly sensitive to the grid size with this more refined treatment of anisotropic turbulence. Note that these correspond to very recent developments that are not implemented in many LES of convective clouds at the present time.

There are some other identified weaknesses associated with turbulence schemes, and more broadly sub-grid-scale processes in LES, notably in the simulation of cloud edges, an example being stratocumulus cloud tops, whose dynamics critically involves fragile combinations of parametrized processes (turbulent and microphysical), grid size and numerical filtering (Stevens et al., 1999, 2005). These have motivated some recent studies which explore these cloud interfaces with DNS (Mellado et al., 2009; Abma et al., 2013).

In the past decades, and still now, numerous CRM simulations have been performed with Smagorinsky-type schemes (e.g. Tompkins and Craig, 1998; Romps, 2008) that were initially designed for finer-grid LES. Klemp and Wilhelmson (1978) were already quite aware of the weakness of this formulation for CRM as the coarser grid size then lies outside of the inertial range. One can guess these authors and others thought that it was premature to deal with this problem at that time and that other difficulties had to be solved first (e.g. the numerics). The study of Bryan et al. (2003) illustrates the sensitivity of the simulation of a squall-line to the grid size (Fig. 5): as the mesh is refined, from 1 km to a LES-type resolution of 125 m, the vertical velocity weakens somehow, in particular, in the stratiform part (to the left); and rainfall decreases (grey shading). However, it is obvious too that the main features of the squall-line are already present in the 1-km simulation. Furthermore, it is important to realize that such simulations are typically influenced to the same extent by the formulation of the microphysics (a simple warm Kessler-type scheme in this study) and its interaction with sub-grid-scale motions. This issue of representation of sub-grid motions in CRMs is also documented by Takemi and Rotunno (2003, 2005) who further emphasize how purely numerical filtering dominates the sub-grid-scale turbulence in their model when using standard values of the parameters involved in the turbulent scheme.

However, even with less numerical filtering and more advanced turbulent schemes (e.g. a prognostic TKE equation is more often considered now), several issues remain. This concerns the simulation of sub-grid-scale moist dynamics (for instance at cloud edges), but not only. In particular, boundary-layer convective thermals (typically a few km wide) are reasonably well resolved by LES but marginally so with the coarser CRM grids; this is a so-called *grey zone* where both resolved and parametrized motions are active, with issues associated with 'work-sharing'. For instance, the atmosphere is very reactive to 'dry' convective instabilities, and if the sub-grid mixing is not strong enough to remove it quickly, spurious thermals can develop instead at the larger resolved scales (Honnert et al., 2011, Fig. 6), which can further lead to unrealistic structures in simulated boundary-layer cumulus clouds (dictated by these resolved boundary-layer motions). In fact, for CRMs, as well as
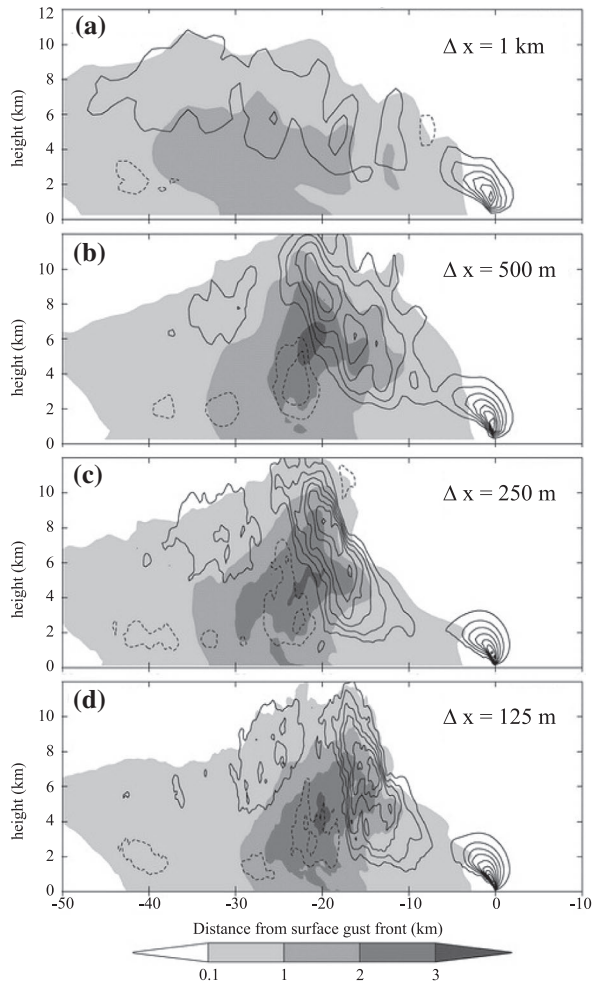
Fig. 5. Horizontal-mean vertical cross-sections of vertical velocity (contour interval 1 m s⁻¹) and rain water mixing ratio (shaded) of squall-line simulations using grid spacing of (a) 1000 m, (b) 500 m, (c) 250 m and (d) 125 m in all three directions, except for (a) where the grid spacing is 500 m on the vertical – adapted from Bryan et al. (2003), ©Copyright 2003 AMS.
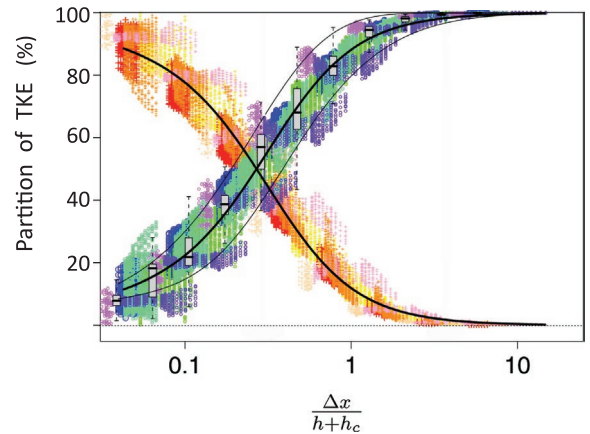

Fig. 6. Relative contributions of the resolved (warm colours) and subgrid (cold colours) motions to the total turbulent kinetic energy (TKE) within various convective boundary layers simulated by LES as a function of the dimensionless mesh $\Delta x/(h + hc)$ where Δx is the LES grid size and $h + hc$ is the height of the cloudy boundary layer. The grey box-and-whiskers plots show the median and the variance of the resolved TKE per class of $\Delta x/(h + hc)$ – adapted from Honnert et al. (2011), ©Copyright 2011 AMS.

4.3. Water phase changes and microphysics

Note that simulations of shallow non-precipitating clouds do not all incorporate an explicit representation of microphysical processes. Instead, condensation and evaporation of water are dictated by a moist thermodynamic adjustment. Thus, cloud water forms when the air is saturated, with the underlying assumption that the concentration of cloud condensation nuclei is large enough so as not to delay condensation. However, microphysical considerations become necessary as soon as one focuses on rain formation, or mixed-phase clouds for instance.

The more frequent formulation of microphysical processes in LES and CRMs is based on an a priori separation of hydrometeors into two main categories: (i) cloud water, including small liquid droplets and ice crystals suspended within the air mass and (ii) precipitating water, either in the form of rain drops, hail, graupels, aggregates or snow, each falling with respect to the air mass. This distinction between different types of hydrometeors is somewhat artificial and arbitrary, especially for ice-phase hydrometeors, and other approaches are explored to move away from these hypotheses (Morrison and Grabowski, 2008). However, as they stand now, current parametrizations of microphysical processes typically include prognostic equations for each retained hydrometeor-type, from a single one (for simulation of non-precipitating clouds) to two (for liquid-phase precipitating clouds) to four or more (for deep convective clouds).

Microphysical processes are numerous and complex, and this translates into exchanges between the different types of hydrometeors; these are controlled by several dozen of parametrized processes when the solid phase is considered, including, among others, condensation, autoconversion, accretion, evaporation,

coarser-grid mesoscale models, local eddy-diffusivity formulations are not well designed to deal with convective boundary-layer turbulence, because it manifests as a non-local process (thermals scale with the boundary-layer depth, irrespective of the smaller grid size) with counter-gradient turbulent fluxes. Local eddy-diffusivity formulations, by design, tend to underestimate such fluxes and cannot reproduce counter-gradient fluxes. In order to solve this issue, non-local schemes (e.g. Troen and Mahrt, 1986; Hong and Pan, 1996) are sometimes implemented (e.g. Wu et al., 1998) and modification of the mixing length has also been proposed (Bougeault and Lacarrère, 1989). More recently, boundary-layer mass-flux schemes (e.g. Hourdin et al., 2002; Neggers, 2009), which provide a more explicit and mechanistic representation of this turbulent process, have been implemented in some CRMs (e.g. Pergaud et al., 2009).
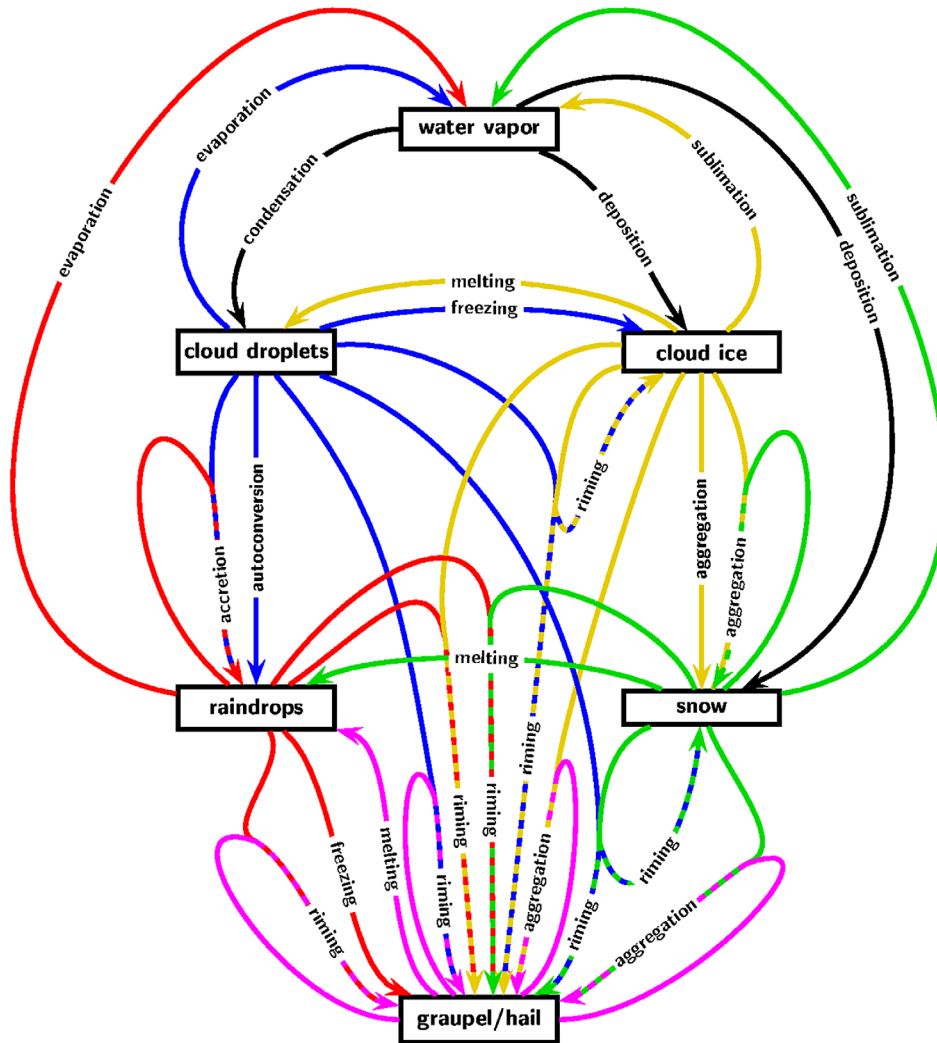
Fig. 7. An example of schematic summarizing for a given one-moment microphysical parametrization, showing the selected water categories or species, with arrows indicating the different processes operating among these species. The colour of an arrow refers to the species that is transformed by a process (black: water vapour, blue: cloud droplets, red: raindrops, yellow: cloud ice, green: snow, pink: graupel/hail), and when two species are concerned, the arrow is two-coloured (© Copyright Axel Seifert, reproduced with permission).

melting, riming, ice initiation and deposition, snow aggregation, sedimentation (e.g. Lin et al., 1983, see also Fig. 7).

A bulk approach is often adopted in current LES and CRMs, which means that particle-size distributions are specified (as opposed to a bin approach that explicitly represents the distribution). A classical example, still in use today, was proposed by Marshall and Palmer (1948) for warm rain, and is expressed as $n(D) = n_0 e^{-\lambda D}$, where n is the density of particles, D the diameter of the particle, λ is referred to as the slope parameter and n_0 as the intercept parameter.[4] Likewise, the parametrization of rain formation proposed by Kessler (1969), which expresses in a simple way the formation of raindrops by autoconversion and accretion of cloud droplets, is also a basis for numerous CRMs in use today.

Microphysical parametrizations are traditionally referred to as single-moment when they incorporate prognostic equations for the mixing ratios of the different hydrometeor types, and as two-moment when they also integrate prognostic equations for particle number concentrations. By design, the latter is more flexible, and better suited for studies focussing on drizzle formation and aerosol-cloud interactions. They do not involve any assumption about saturation adjustment, so they permit the existence of over-saturation that is largely observed for ice. LES of shallow warm clouds now often make use of two-moment schemes (e.g. Khairoutdinov and Kogan, 2000; Seifert and Beheng, 2006). Attempts to introduce these more complex schemes in CRM simulations of deep convection exist (Meyers et al., 1997; Milbrandt and Yau, 2005; Phillips et al., 2007), they

notably point to a sensitivity of rainfall evaporation and convective cold pools to these one- vs. two-moment formulations (Morrison et al., 2009).

More broadly, behind these important distinct features among models, there still exists a wide diversity in the content of microphysical schemes in LES and CRMs, from the specification of hydrometeor types (e.g. particle size distributions, mass–diameter relationships), the types of processes taken or not taken into account, or their formulation. Overall, this field is still the object of active research and numerous studies performed in the past decade show that LES provide a valuable platform to test and implement new parametrizations of microphysical processes (Larson et al., 2002). Furthermore, they allow exploring the sensitivity of clouds to these processes within a dynamic framework where they actually interact with small-scale turbulent motions (Stevens and Seifert, 2008). On the other hand, when using a LES or a CRM, the choice of an appropriate microphysical scheme may appear delicate, however the goal of the study can frame the level of sophistication of the scheme to some extent. For instance, when focussing on convective cold pools and precipitation, it is worth keeping in mind that these features are sensitive to the size and fall speed of rain droplets as noted above. Likewise, processes driving the formation and dissipation of cloud ice are also important for cloud radiative effects.

Cutting the atmosphere into grid meshes introduces artificial discontinuities in the operation of cloud processes, especially if one assumes that each grid box can only be either unsaturated or saturated. In other words, there is no consideration of sub-grid-scale microphysical processes nor of any partial cloud cover that could interact with radiation. This 'all or nothing' hypothesis can become quite unrealistic, for instance the resolution of a CRM does not allow an explicit representation of shallow cumulus clouds. In this case, clouds may well develop, but typically later and too big from the outset, as dictated by the numerics. The existence of thresholds in microphysical parametrization (e.g. Kessler rainfall scheme) also introduces a sensitivity of the results to the resolution. In order to limit such numerically-driven sensitivities, parametrizations have been developed which account for sub-grid-scale processes, i.e. turbulence and microphysics, with a partial cloud cover that can be inferred from the latter. Second-order schemes are formulated in terms of sub-grid-scale variances and covariances of thermodynamic and dynamic fields. In the past, Gaussian distributions have often been assumed (e.g. Sommeria and Deardorff, 1977; Mellor, 1977), and several studies are still working now at improving the realism of these distributions (Golaz et al., 2002; Bogenschutz et al., 2010).

4.4. Radiative processes

It may appear surprising that numerous LES and CRM cloud simulations have been, and still are, performed without much consideration of radiative processes. In fact, this appears as a reasonable assumption in some cases, for instance, for the simulation of short-term internal dynamics of cumulonimbus clouds, because for such phenomena the radiative heating rates are typically of much smaller magnitude than convective processes. However, as soon as one aims to perform simulations over longer time scales (typically more than a few days), or focus on some types of convective clouds (e.g. stratocumulus or ice anvils), the neglect of radiative processes and of their interactions with convective motions and microphysics can become dubious.

The formulation of radiative processes in LES and CRMs spans very diverse flavours and ranges of accuracy, in part as a result of the important amount of computing time required by the parametrization of this process, but also for methodological purposes. For instance, let's consider a simulation of daytime boundary-layer clouds over land using prescribed surface sensible and latent heat fluxes at the lower boundary. It is frequent practice to neglect atmospheric radiative processes in such simulations (e.g. Neggers et al., 2003a)[5]. However, even if the *direct* interactions of radiative processes with atmospheric motions and clouds are not taken into account, still their (major) imprint on the surface-driven boundary-layer growth is expressed in surface turbulent heat fluxes, as the surface energy balance dictates that the sum of these fluxes equates net radiation minus the ground heat flux (i.e. $H + LE = R_{net} - G$, where H and LE are respectively, the surface sensible and latent heat flux, G the ground heat flux and R_{net} the net radiative flux at the surface).

The presence of transient clouds largely affects radiative cooling rates in both the shortwave (SW) and longwave (LW) ranges at small time and space scales. However, one can recall that a daily-mean value is typically 1 K.day^{-1}. Thus, radiative processes actively contribute to the atmospheric heat balance at scales of a few days and more when temperature does not fluctuate much, such as in the tropics. This radiative constraint is sometimes introduced in a very simple way (e.g. Robe and Emanuel, 1996; Muller et al., 2011). In both studies, CRM simulations are carried out over tens of days to mimic convective equilibrium states over ocean using fixed SST and constant radiative cooling rates in the absence of any larger-scale advection. Basically, such a setup ensures that convective activity does not cease and helps to prevent temperature and moisture drifts that could otherwise occur. Note however that prescribed constant cooling rates as large as 5 K day^{-1} are sometimes found in the literature, but such rates are much stronger than indicated by physically-based considerations of radiative processes. More fundamentally, by design, such simplification excludes the operation of any cloud-mediated convective-radiative interactions.

Even when interactions between cloud and radiative processes are critical to the cloud dynamics such as for stratocumulus, simplified or empirical formulations are sometimes employed

to relate radiative heating rates to liquid-water mixing ratios. For instance, Stevens et al. (2005) made such a choice because it was better suited for a LES intercomparison whose object was not to explore the sensitivity of the results to the parametrizations of radiative processes as such. In the past 20 years, more sophisticated parametrizations of radiative processes have been progressively introduced in several LES and CRMs, but mainly in order to account for the cloud reflection, absorption and scattering of radiation. They often resemble parametrizations used in large-scale models, with separate formulations of longwave and shortwave radiation (with major control of scattering in the SW, whereas emission and absorption dominate in the LW). As in large-scale models, these radiative transfer schemes also consider a limited number of spectral bands (referred to as broadband schemes). They usually make use of the two-stream approximation, whereby the radiative flux divergence is expressed in each band as a difference between an upwelling and a downwelling radiative flux, and these fluxes are computed independently for each model column (with no horizontal exchanges). Note that the situation is conceptually simpler in CRMs and LES than in large-scale models because the cloud field is now almost fully resolved; the overlap assumptions, which are needed to decide how to arrange the different cloud layers within a column, are therefore only relevant to the remaining columns that contain grid cells where the cloud cover is less than unity (and then only when a sub-grid cloud cover is parametrized).

Unlike in large-scale models, where precipitating hydrometeors are often removed from the atmosphere by parametrized convection as soon as they form, precipitating hydrometeors are explicitly simulated in LES and CRMs and remain some time in the atmosphere before they reach the surface or experience evaporation for instance, so that they can, in principle, participate in radiative transfer. However, their impact is often neglected and only the radiative properties of cloud liquid drops and ice crystals (plus sometimes drizzle and snow) are taken into account.

The impact of clouds on radiation is dependent on the size distribution, shape and concentration of the hydrometeors they are made of. Thus, the radiative properties of near-spherical liquid drops are typically better ascertained than those of ice particles, which display wide variations in shapes and sizes, even within a single cloud.

Practically, shortwave radiation schemes include a formulation of the optical thickness (σ), single scattering albedo (ω)[6] and asymmetry factor (g)[7] in cloudy pixels for each separate band. These three variables are most often expressed as a function of the liquid or ice cloud-water path (*CWP*) and of an effective radius (r_e)[8], following some parametrizations used in large-scale models (e.g. Slingo, 1989; Ebert and Curry, 1992; Fu, 1996). For instance, in Slingo (1989) and Ebert and Curry (1992), they are expressed as:

$$\sigma_i = CWP \left(a_i + b_i / r_e \right)$$

$$1 - \omega_i = c_i + d_i r_e$$

$$g_i = e_i + f_i r_e$$

where the subscript i refers to the ith spectral band and a_i, b_i, c_i, d_i, e_i and f_i are fitted parameters. Note that simpler parametrizations that only retain a dependence on the cloud-water path have also been proposed (e.g. Sun and Shine, 1995).

For longwave radiation, in the simplest case, scattering is neglected and clouds are treated as grey bodies with an emissivity parametrized as $\varepsilon = 1 - e^{-\alpha\,LWP}$, where α is a constant on the order of 0.15 (Stephens, 1978). Typically a thick convective cloud behaves almost like a black body with $\varepsilon \sim 1$, unlike a thin cirrus cloud which has an ε less than 0.5. Note that more refined parametrizations have been developed that also account for the not-always-negligible impact of cloud scattering in the longwave (e.g. Fu et al., 1998).

A basic issue with the use of such parametrizations in models is that they were developed for specific types of clouds, sometimes designed with the help of a few experimental data, and they may not be as appropriate when applied to other cloud types. In addition, for those parametrizations where the effective radius r_e is an input variable, some ad hoc choices are sometimes made (e.g. in the simplest case a fixed value of r_e), without any direct connection to the parametrization of cloud microphysics. Even if someone is not working specifically on these different schemes and on their interactions, it can turn out to be important to know about these 'details' in order to correctly interpret simulations and their sensitivities.

Finally, one must also realize that the underlying assumptions of two-stream parametrizations become less and less valid as the geometries of clouds depart more from sheets of plane parallel layers (e.g. cumulus clouds). In fact, the few studies assessing how such simplified formulations compare to fully three-dimensional radiative transfer computations in cloudy skies tend to support the usefulness of two-stream parametrizations (Pincus, 2013). Still, the integration of computationally-expensive radiative processes in high-resolution LES of clouds brings numerous challenges (e.g. Pincus and Stevens, 2009). Indeed, only a few attempts have been made to include 3D radiative effects in CRMs (e.g. Wapler and Mayer, 2008; Klinger and Mayer, 2016; Jakub and Mayer, 2016).

4.5. *Initial and boundary conditions and their significance for limited-area modelling*

Intuitively, one understands the importance of the initial conditions to the modelling of atmospheric cumulus clouds. For instance, the vertical development of deep convective cells are constrained by the atmospheric stability and tropopause height, while their morphology is strongly shaped by the wind field, notably the vertical shear. However, the choice of boundary conditions is often as crucial, even for short-duration (less than a day) runs, and it must not be overlooked when designing LES

or CRM simulations. So far, we discussed the need to properly represent sub-grid-scale turbulent motions (together with the physical processes and their couplings). However, LES and CRM results are also naturally quite sensitive to larger-scale motions as well, and the latter are set or specified by the choice of lateral boundary conditions.

In part, this sensitivity to initial and boundary conditions reflects the influence of large-scale states and circulations on convective processes and, to quote a common expression, is sometimes interpreted as 'the *response* of convection to larger-scale processes'. Still, this sensitivity can also express the strong interactions arising between convection and the larger-scale environment, and they can be quite fast in terms of vertical motions once deep convection starts to operate.

As a kind of rule, people designing and using LES and CRMs have often tried to formulate initial and boundary conditions that are well suited to the purpose of the simulations, while remaining as simple as possible. Below, we successively recall commonly used initial and boundary conditions, the latter comprising lateral, bottom (surface) and top of the domain boundary conditions (summarized in Fig. 8); these are not exclusive, other choices can be imagined as long as they are meaningful and suited to the purpose of a simulation.

A simple and frequent choice is to initialize the simulation with atmospheric profiles applied homogeneously to each vertical column of the domain, a domain whose horizontal size is typically less than the scales of fluctuations in the free troposphere (at least for calm, non-convective conditions). In doing so, depending on the purpose of the simulation, profiles of temperature, moisture and horizontal wind can be derived from a sounding, or designed from more academic considerations. The initialization of vertical velocity and cloud-water contents is more challenging (a simple choice is to set them to 0, sometimes referred to as a 'cold start').

From these horizontally-homogeneous initial profiles, small-scale motions are often initiated by some noise applied at the low levels. However, the simulation of convection with this approach can be unsuccessful when the sources of convective instability (e.g. surface boundary conditions and more specifically surface fluxes, radiative processes, vertical motions) are not well taken into account. This is typically the case for the simulations of deep convection that ignore surface heat fluxes, and it may happen that deep convection never occurs or only after several hours of simulations, in an environment that has drifted too much from the initial state. This is the main reason why in some simulations of deep convection, warm or cold 'bubbles' are 'added' to the initial homogeneous vertical structure. These are typically less than one km deep and one to a few km wide and aim to mimic in an academic way the triggering of convective cells by a thermal or a gravity current (Klemp and Wilhelmson, 1978; Bryan et al., 2003; Yeo and Romps, 2013). Once initiated, for instance with a line of cold bubbles, these deep cells can feed in turn a cold pool and thus, further sustain deep convection. Such a simulation setup is well suited to study a deep convective event in its mature stage. However, by design, it precludes investigations of the mechanisms of convective initiation, as these are enforced by the initial bubbles.

Finally, note that the real atmosphere is turbulent, not horizontally homogeneous. Therefore, when a simulation is initiated with such an approach (with either random noise or isolated bubbles added), a certain amount of time is necessary for realistic turbulent, convective motions to develop; this is the spin-up period. Its length depends on the time scale of the processes under study; for instance, it is reasonable to discard the first hour of simulation – which corresponds typically to a few turnover times – when focussing on convective boundary-layer processes.
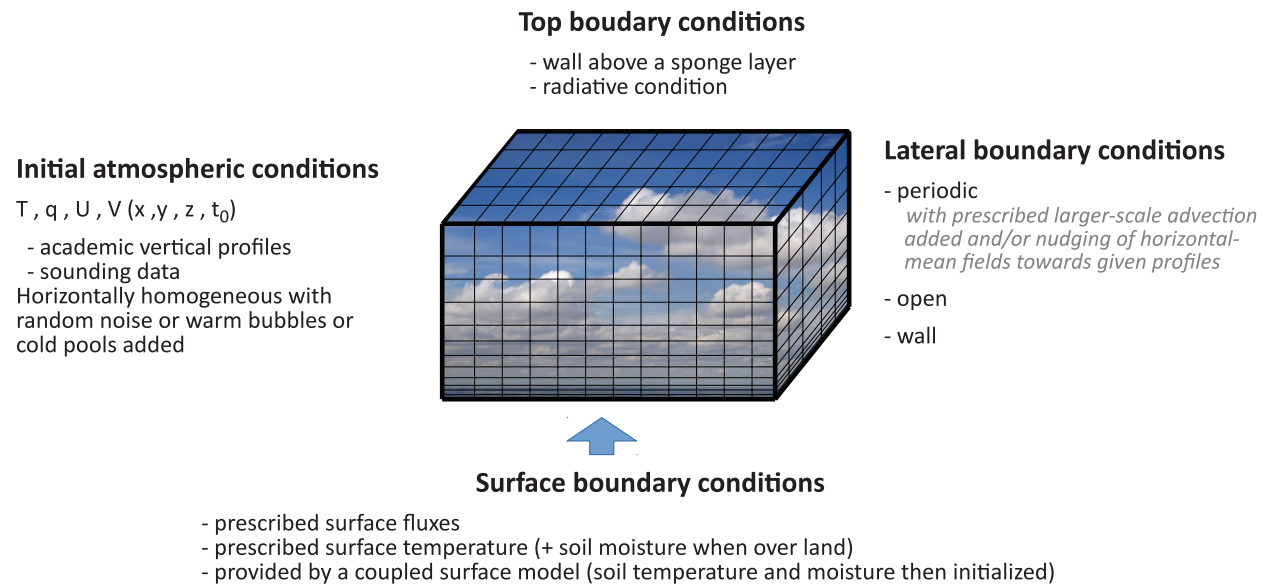
Top boudary conditions
- wall above a sponge layer
- radiative condition

Initial atmospheric conditions

T , q , U , V (x ,y , z , t$_0$)

 - academic vertical profiles
 - sounding data
Horizontally homogeneous with random noise or warm bubbles or cold pools added

Lateral boundary conditions

- periodic
    with prescribed larger-scale advection added and/or nudging of horizontal-mean fields towards given profiles

- open

- wall

Surface boundary conditions
- prescribed surface fluxes
- prescribed surface temperature (+ soil moisture when over land)
- provided by a coupled surface model (soil temperature and moisture then initialized)

Fig. 8. Schematic of common choices of initial and boundary conditions in LES and CRMs.

Both LES and CRMs are limited-area domains, therefore lateral boundary conditions are required. The two most common choices are periodic and open lateral boundary conditions. The former is well suited to numerically explore the behaviour of a convective phenomenon of relatively large spatial extent which displays regular mesoscale patterns. For instance, when focussing on wide decks of stratocumulus or shallow cumulus fields extending over hundreds of km, it can be both convenient and meaningful to choose to simulate a small piece of it, thus viewed as a part of a wider homogeneous system, with periodic lateral boundary conditions (note however that the horizontal domain of simulation must be large enough to contain the cloudy patterns of interest). In the case of periodic boundary conditions along the x-direction for instance, each variable a must satisfy the following, involving the two x-axis borders, for each point y along the y-axis, and at all vertical levels z and time steps t: $a(x_{n+1}, y, z, t) = a(x_1, y, z, t)$, where n is the number of points along the x-axis, and x_{n+1} is a fictitious point introduced here for numerical purposes.

A direct consequence of this major constraint is induced by mass conservation: it means that the net horizontal divergence of fluxes across the domain and the mean vertical velocity are both zero at all heights. When this assumption corresponds to an unrealistic hypothesis with detrimental effects, a formulation of larger-scale horizontal and vertical advection is often introduced as in Sommeria (1976) or Grabowski et al. (1996). The latter in particular provides a comprehensive presentation of the separation between larger (prescribed) and smaller (simulated and parametrized) scales of motions and fluctuations underlying such derivations. In short, additional terms are introduced into the budget equations of temperature and water variables, for this larger-scale advection, in the form:

$$\left(\frac{\partial \overline{\alpha}}{\partial t}\right)_{LS} = -W_{LS}\left(\frac{\partial \alpha_{LS}}{\partial z}\right) - \left[U\left(\frac{\partial \alpha}{\partial x}\right) + V\left(\frac{\partial \alpha}{\partial y}\right)\right]_{LS}$$

These profiles are then applied homogeneously to all columns of the simulated domain. For instance, a large-scale subsidence is often introduced in LES of subtropical shallow cumulus clouds, and combined with the horizontal-mean profile of simulated α, to formulate the effect of the large-scale vertical advection associated with this subsidence (corresponding typically to a mean warming and drying). The additional large-scale term can also be used to prevent unrealistic thermodynamic drifts that can arise when the sources of energy into the system (surface fluxes and radiation) are not balancing each other (in terms of equivalent potential temperature, or equivalently, moist static energy). It is also used in simulations of deep convection carried out over large domains where larger-scale advection corresponds either to an academic setting or is inferred from observations or meteorological analyses (Grabowski et al., 1996). In this periodic configuration, the large-scale control on the wind field

is often taken into account via a nudging of the horizontal mean wind to given wind profiles or, less often, to a geostrophic wind component (when the Coriolis force is considered) that cannot be represented in the absence of large-scale horizontal pressure gradients. Implicit to this choice is the assumption that the mean wind is largely governed by the larger-scale dynamics, and must therefore be prescribed. This is especially important if one wants to reproduce the spatial patterns of convective clouds (for instance, cloud streets, scattered deep convection vs. squall-lines, anvils) which are strongly dependent on the mean wind field. This can also be critical to surface energy exchanges, especially over ocean (Redelsperger et al., 2000b).

Recently, a quite distinct formulation of larger-scale circulations was introduced in CRMs using periodic lateral boundary conditions. It is referred to as the weak temperature gradient (WTG, Sobel and Bretherton, 2000) and was motivated by the uniformity of temperature profiles observed in the oceanic tropics, close to the Equator. In short, it consists in prescribing a temperature rather than a mean vertical velocity profile in the larger-scale advection term. Thus, in CRMs with periodic lateral boundary conditions, this translates into a mean temperature nudged towards a given profile, which in turns dictates the fluctuations of vertical advection (Raymond and Zeng, 2005; Daleu et al., 2015). In its simplest form it can be formulated in a CRM using periodic conditions as:

$$\left(\frac{\partial \overline{\theta_v}}{\partial t}\right)_{LS} = -w_{LS}\left(\frac{\partial \overline{\theta_v}}{\partial z}\right) = -\frac{f(z)}{\tau}\frac{\overline{\theta_v} - \theta_v^{REF}}{\partial t}$$

where θ_v^{REF} is a reference virtual temperature profile, τ a time constant (typically taken equal to a few hours) and $f(z)$ a weighting function which varies with height (e.g. to prevent adjustment in the sub-cloud boundary layer). A joint, similar formulation for the large-scale advection of specific humidity (thus involving a reference profile for water vapour too) is sometimes introduced (Daleu et al., 2015).

While very different by design from the open lateral boundary conditions presented just below, this WTG framework, in its spirit, also allows more freedom in the development of convective processes. Indeed, these processes notably dictate the larger-scale vertical velocity field, while it was prescribed in the previous equation.

Periodic conditions are not the best suited for the simulation of all convective phenomena. For instance mature squall-lines, which develop as isolated mesoscale systems displaying cloud shields up to several hundreds of km wide, are generally better apprehended by models using 'open boundary conditions'; the aim there is to build somewhat 'transparent' boundaries. In that case, the evolution of the larger scales of motion are not prescribed, but instead tend to passively 'respond' to convection arising within the domain, and typically an inflow

of air develops in the lower troposphere and an outflow above. Note that some care is needed though in the formulation of this type of open conditions in order to minimize wave reflection at the lateral boundaries (e.g. Klemp and Wilhelmson, 1978; Carpenter, 1982). It is also important to properly define the characteristics of the air entering the domain. A major difference with periodic boundary conditions arises in the budget equations, because the horizontal mean vertical velocity, largely controlled by convective processes developing inside the domain, departs from 0 and generally accounts for substantial vertical advection. Such simulations are generally carried out over a few to several hours to study specific deep convective systems.

Finally, lower and upper boundaries are also needed and they are generally kept simple in CRMs and LES. Both of them often consist of rigid lids ($w = 0$). The lower boundary is generally assumed to be flat (see Kirshbaum and Grant (2012) for an example of non-flat lower boundary).The upper bound is typically set a few to several km above the atmospheric layer under study, and an absorbing layer, or sponge layer is often introduced below the domain top. In this layer, typically a few km deep, a nudging towards prescribed profiles is added to the prognostic equations in order to damp wave reflection at the top of the domain (e.g. Clark, 1977; Durran and Klemp, 1983; Redelsperger and Lafore, 1988).

The choice of the lower boundary is generally a more important issue, because it conditions the formulation of surface fluxes, which in turn strongly control the magnitude of boundary-layer turbulence. Over ocean, a common simple choice is to prescribe values of SST together with bulk formula for surface fluxes. To explore ocean-atmosphere interactions arising at the mesoscale, a mixed layer of the surface water was implemented in a few studies (e.g. Wu et al., 1998; Esau, 2014). Sullivan et al. (2014) also analysed the sensitivities of the atmospheric boundary layer to marine waves. However, the explicit modelling of ocean-atmosphere interactions at the mesoscale has not received much attention yet. Likewise, over land, it is common practice to assume that the surface is flat, and to prescribe surface sensible and latent heat flux, together with a roughness length. Land-atmosphere couplings just start to be addressed with LES (Patton et al., 2005; Lohou and Patton, 2014), and this again requires the coupling to a land-surface model (LSM). The LSM can be kept relatively simple (the Penman-Monteith model is an example of a very simple LSM) or adapted to address particular issues. Note that clouds have a strong impact on the surface energy budget. This impact is observed in the longwave radiation at night, especially when the atmosphere is dry. Clouds also profoundly affect the incoming shortwave radiation during daytime, and such a coupled modelling framework may prove to be very helpful to study interactions between surface, boundary-layer and convective cloud processes.

5. A few examples of results

5.1. Simulations and their evaluation

It is not possible to summarize here the range of simulations performed with CRMs and LES; they range from purely academic to strongly observationally-constrained. Indeed, they are used for numerous purposes, to help address a very wide range of scientific questions. Still, evaluating simulations is always necessary, especially as questions become more and more demanding for models. In this respect, dedicated observational campaigns provide the opportunity to test numerical simulations against the real world, and these have been widely used, from the 70s until now. Because of the transient nature of convective phenomena they often focus on statistical properties of cloudy convective boundary layers, on the scales (in time and space) and magnitude of convective features, e.g. distribution of in-cloud vertical velocities (Khairoutdinov et al., 2009) or comparisons of cloud field distributions in LES and observations (Neggers et al., 2003b; Corbetta et al., 2015). Radar data are also very helpful to assess the microphysics and internal dynamics of deep convective systems (Brown and Swann, 1997; Lafore et al., 1988; Feng et al., 2015). Such studies are important, though not straightforward, and much caution must be used in the design of the evaluation approach, as uncertainties in the initial and boundary conditions can cause departures from observations which are not related to the physics or numerics of the model. This also reflects the inherent difficulties of observing transient intermittent cloud processes. Conversely, note that when simulations are sufficiently close to observations, they can help to complement data. For example, Oue et al. (2016) used LES 3D results to help understanding and correcting biases in observational cloud fraction estimated from vertically-pointing remote-sensing instruments.

As more and more observations become available (e.g. high-frequency and resolution satellite data, long-term data-sets from observatories sampling different climatic regions), there is a constant renewal in the utilization of observations in LES and CRM studies. These range from new types of model evaluations to modelling studies aimed at solving the numerous questions raised by these observations. For instance, the recent LES performed by Heinze et al. (2017) over a notably wide domain (around 700–1000 km) motivates other types of comparisons with high-resolution satellite data. It becomes possible to analyse whether the simulation is able to reproduce the contrasted spatial distribution of clouds and to explore the relevance of the simulated mechanisms (e.g. the coexistence of rolls and cells in the domain, the varied sizes of shallow cumulus, the potential influence of gravity waves (Clark et al., 1986).

A frequently used and complementary evaluation of LES and CRM started in the 80s as several of these models were then developed and used across the world: it consists in model intercomparison, where simulations are performed with different

models (with distinct numerics and physical parametrizations) using close setups (in terms of domain size, resolution, time of simulation and wherever possible initial and boundary conditions). Such intercomparisons are the only way to assess whether different models provide (or not) similar behaviour of major variables that are at best partly obtained from observations (for instance, turbulent and convective fluxes, cloud statistics), but critical for the development of process-based parametrizations in large-scale models. Several intercomparisons of this type have been carried out, for both shallow and deep convective clouds, mostly over ocean (Redelsperger et al., 2000a; Stevens et al. 2001, 2005; Siebesma et al., 2003; van Zanten et al., 2011; de Roode et al., 2016), with only a few over land (Brown et al., 2002; Xu et al., 2002; Guichard et al., 2004).

Intercomparisons of LES of shallow cumulus clouds generally indicate a good agreement for mean variables and flux profiles. However, some issues remain, in particular, for the representation of turbulent kinetic energy, cloud tops and precipitation fluxes (Stevens et al., 2001; Brown et al., 2002; Siebesma et al., 2003; van Zanten et al., 2011; de Roode et al., 2016). The simulation of stratocumulus (e.g. Stevens et al., 2005) and deep convective clouds is more challenging. Figure 9 illustrates one of these intercomparisons for the simulation

of a mature squall-line (Redelsperger et al., 2000a). The four CRMs simulate relatively close spatial structures of the convective system, with a convective line at the front (on the left) and a more stratiform region behind; the overall structure is consistent with observations (Fig. 9a). Note however the lower magnitude of rain water in the fourth CRM (Fig. 9b4)). This departure is largely related to the formulation of the lateral boundary conditions (it was the only simulation using periodic instead of open conditions, and the zero horizontal-mean vertical velocity weakened deep convection in this simulation compared to the others). Note also that the size of the fine-scale convective structures is sensitive to choices in the numerics and physics (e.g. Takemi and Rotunno, 2003, 2005) and this very likely plays a part in the differences among simulations here. An example of this type of sensitivity is given in Fig. 10.

Results from another intercomparison study are provided in Fig. 11 (from Xu et al., 2002). In this case, the simulations were more energetically constrained, with periodic boundary conditions and prescribed surface sensible and latent heat fluxes (i.e. unlike in the previous example, the fluxes of heat and water vapour into the system, from the surface and the larger-scale circulations, were exactly the same in all simulations). This configuration is also generally used for LES intercomparison.
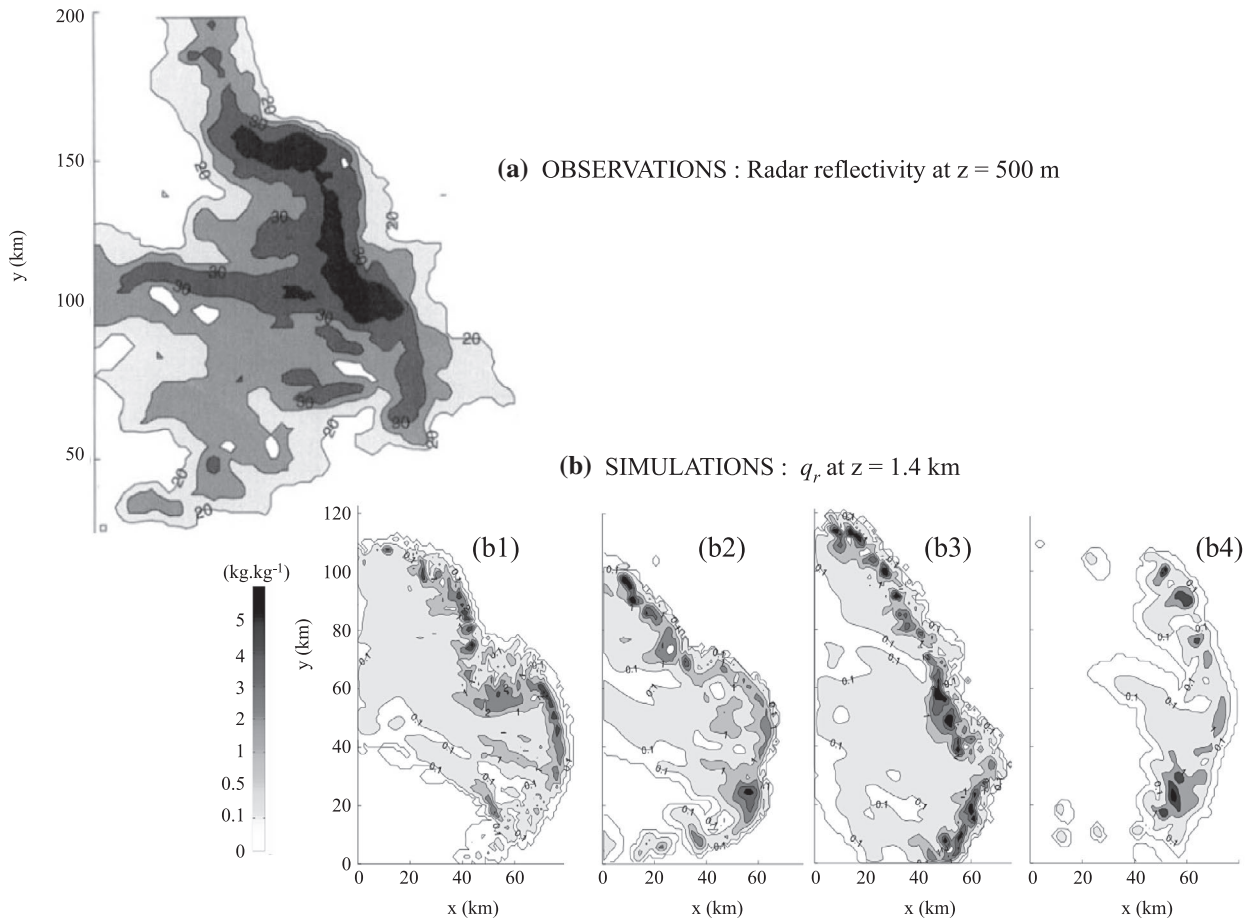

Fig. 9. Intercomparison of simulations of a mature squall-line performed with four distinct CRMs: the horizontal structure of the observed convective system is shown with a cross-section of radar reflectivity at 500 m above the surface in (a) and with simulated specific rain water (qr) at 1.4 km above the surface (b1–b4) – adapted from Redelsperger et al. (2000a), © Copyright 2000 Royal Meteorological Society (RMS).
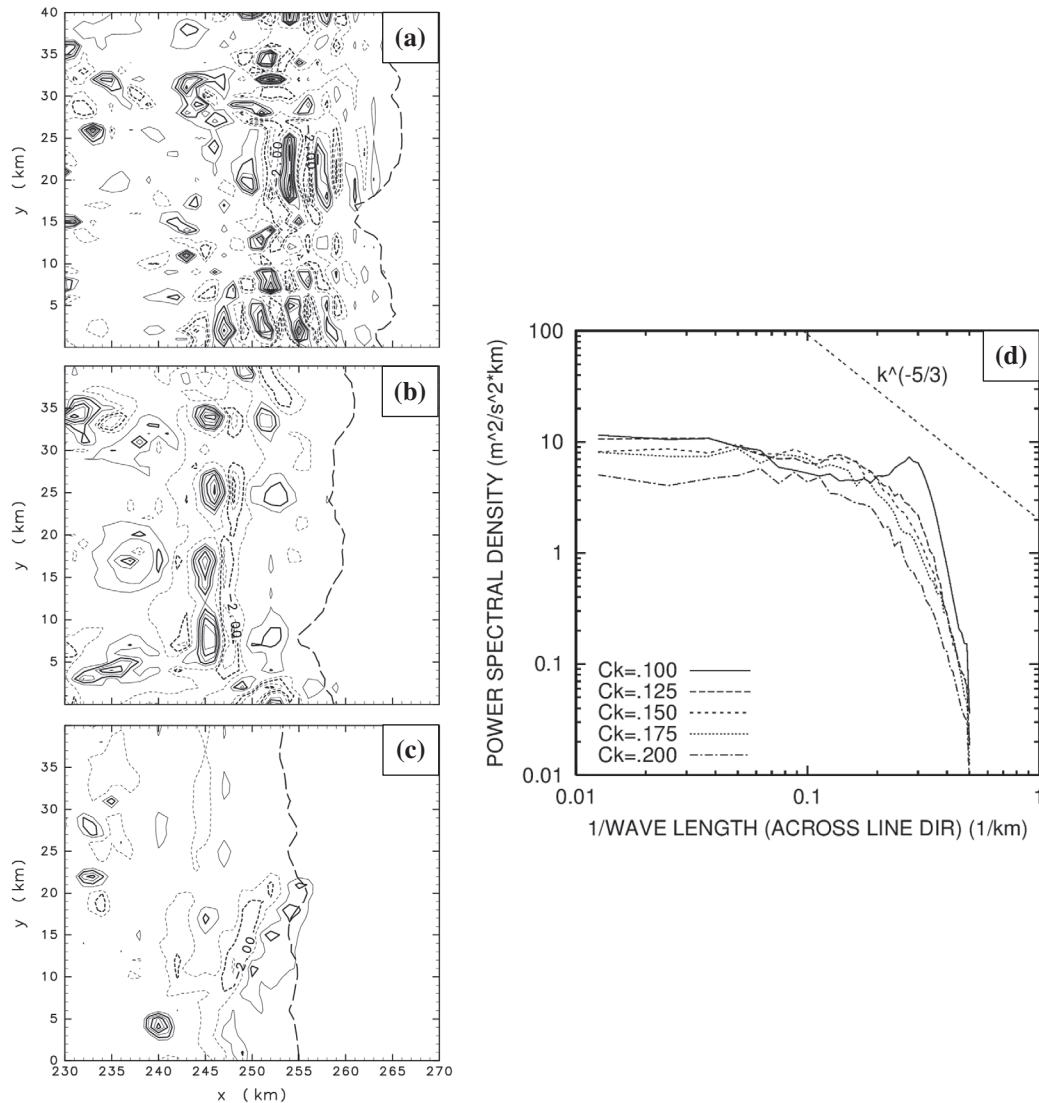
Fig. 10. Horizontal cross-sections of vertical velocity at 3 km above the surface in squall-line simulations differing in the choice of the constant Ck appearing in the formulation of the eddy diffusivity of the turbulent scheme ((a): *Ck* = 0.1, (b): *Ck* = 0.15, (c): *Ck* = 0.2). In these cross-sections, the dashed line corresponds to the gust front, and the interval between isolines is 1 m s^{-1}. They choice of Ck has an impact on the number, intensity and scale of the simulated convective cells: they become spuriously small, strong and numerous for *Ck* = 0.1, while the opposite is observed for *Ck* = 0.2. The corresponding power spectra density (d) shows that the spurious peak of energy building up at short wavelengths for *Ck* = 0.10 (solid line) disappears for higher values of Ck – adapted from Takemi and Rotunno (2005), © Copyright 2005 AMS.

It illustrates the magnitude of the mean thermodynamic biases that can be expected from this type of simulation. The similar vertical structures of the biases across models again suggests an influence of the common boundary conditions. On the other hand, the left panel indicates that all models provide rather close profiles for the convective updraught and downdraught (i.e. variables that are not currently available from observations), and emphasizes the significance of the convective downward mass flux, an expected feature in this case portraying deep convective events over land. There is relatively more scatter in the downdraught profiles, and this is again expected as the dynamics of

downdraught, strongly controlled by rain evaporation, relies more heavily on the parametrization of microphysics than the dynamics of updraught which is controlled to a first order by the thermodynamics of phase changes.

Overall, numerous model intercomparisons have pointed to much better agreement among the depiction of convective cloud processes in LES and CRMs than obtained with parametrized models, in terms of mean structures, as well as timing (e.g. phase in the diurnal cycle, Guichard et al., 2004). As a result, the robust 'non-observable' outputs of the simulations turn out to be very helpful in the development of more
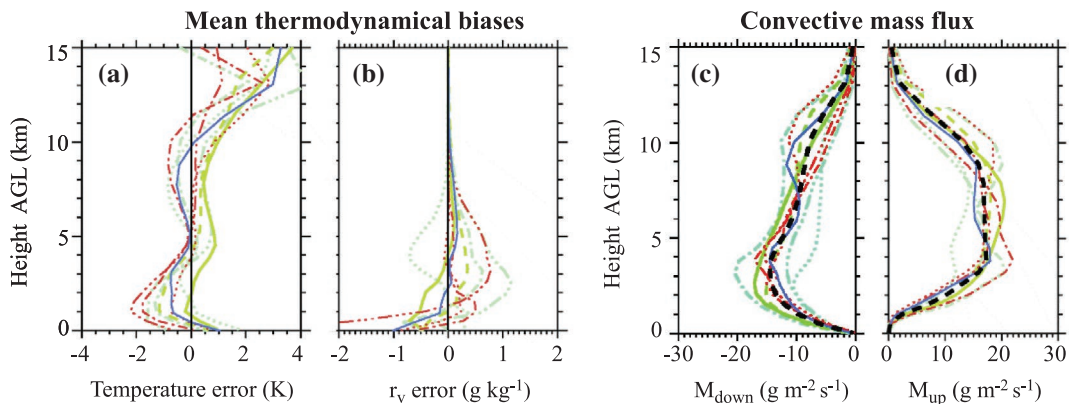
Fig. 11. Intercomparison of CRM simulations of 14-day mean profiles of temperature (a) and (b) water vapour mixing ratio biases relative to observations and convective downdraught (c) and updraught (d) defined in the same way in each run – each line corresponds to one model and the thick dashed lines in (c) and (d) are the average of CRM profiles – adapted from Xu et al. (2002), © Copyright 2002 RMS.

physically-based parametrizations, and these are now widely used for this purpose (see Section 5.4).

5.2. Insights into convective clouds phenomenology and process understanding

As discussed above, the causes behind numerous observed cloud patterns (open and closed cells, cloud streets, structuring – or aggregation – of deep convection in mesoscale multi-cellular deep convective systems, their orientation) are not all very well understood (Etling and Brown, 1993; Atkinson and Zhang, 1996; Cotton et al., 2010). In the last decades, several studies have tried to reproduce and study these structures with LES and CRM. A few, very much non exhaustive, examples of such studies are briefly presented below.

Satellite data reveal the ubiquity of shallow cloud patterns, which appear somewhat similar to Rayleigh–Bénard convection which develops above a critical Rayleigh number within a fluid located between two plates and heated from below. In a cloudy atmosphere, fields of shallow cumulus trace the presence of boundary-layer open cells (with updraught and cloud at the centre) or rolls (cloud streets, often aligned with the mean winds (LeMone and Pennell, 1976; Weckwerth et al., 1996), while stratocumulus fields are primarily associated with closed cells over ocean (with upward motion along the cell edges) (Wood, 2012). However, in contrast with laboratory experiments and theoretical linear models, the aspect ratio of cell diameter to cell height is typically much larger in the atmosphere (around 20:1) instead of 1:1, i.e. they are much flatter. Furthermore, observed mesoscale cells often involve more than one cumulus cloud (Cotton et al., 2010).

Müller and Chlond (1996) were among the first to explicitly simulate and analyse the broadening of cells during a cold-air outbreak (because of computation limitation, they progressively increased the size of the grid mesh and of the domain in order to be able to simulate mesoscale cellular convection patterns).

With the help of sensitivity experiments, they showed that diabatic heating sources, namely condensation and cloud-top radiation were major drivers of cell broadening. These results were further supported by the LES experiments of Schröter et al. (2005). Latent heat release associated with drizzle formation and large-scale dynamics have also been invoked to explain the large aspect ratio of mesoscale cellular convective elements in fields of stratocumulus clouds (Xue et al., 2008; Savic-Jovic and Stevens, 2008). However, the representation of precipitation in stratocumulus is challenging and the size of the observed pattern is demanding in terms of computing power. Recently, the role of atmospheric aerosols has also been highlighted as controlling the formation of precipitation and therefore the mesoscale organization of stratocumulus fields (Wang and Feingold, 2009). Feingold et al. (2010) showed that the concentration of atmospheric aerosols could control the horizontal patterns of stratocumulus fields, from closed cells for large aerosol concentrations associated with weakly precipitating clouds to open cells for small aerosol concentrations associated with precipitating clouds (Fig. 12). In the open cells, strong updraught are present on the cell walls. In such thick clouds, precipitation forms and falls. While falling, the evaporation of the precipitation induces cooling and the formation of outflows which favour moist convection in other locations when they collide.

Observations also show transitions of regimes in space and time: from closed to open cells over tropical oceans (stratocumulus to cumulus transition taking place over wide regions from the subtropics to the tropics, Albrecht et al., 1995), and from rolls to open cells from the morning to the afternoon over land (Weckwerth et al., 1999) or during cold air outbreaks (Brümmer, 1999). Over land, this transition has been related to the fact that the thermal instability becomes dominant over the dynamic instability as surface sensible heat fluxes increase. This appears reasonably well simulated with LES (Liu et al., 2004; Lothon et al., 2007). The stratocumulus to cumulus transition over tropical oceans have also been extensively studied
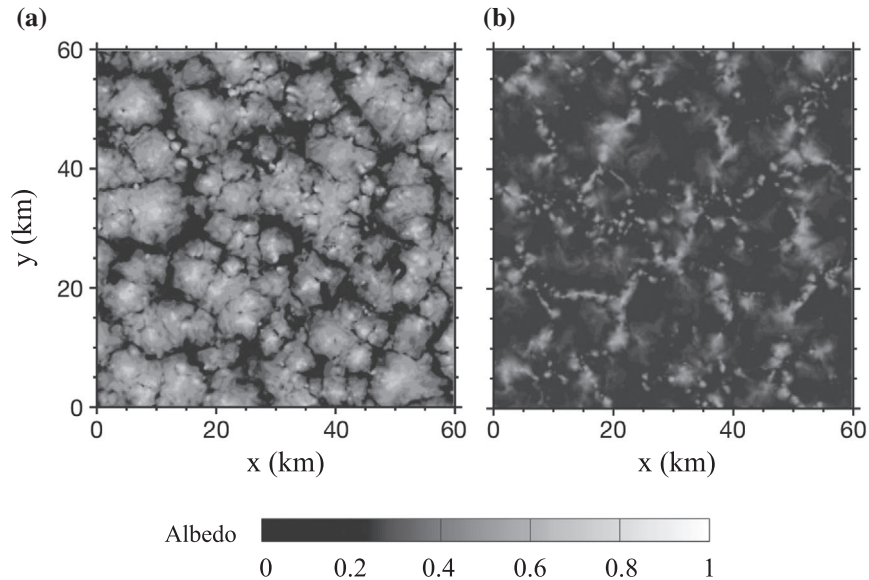
(a) **(b)**

Fig. 12. A snapshot of cloud albedo associated with (a) closed and (b) open cellular structures simulated with LES. The two simulations only differ in the initial concentration of aerosol with a high concentration favouring non-precipitating clouds in (a) and a low concentration favouring drizzle in (b) – adapted from Feingold et al. (2010), © Copyright 2010 Nature.
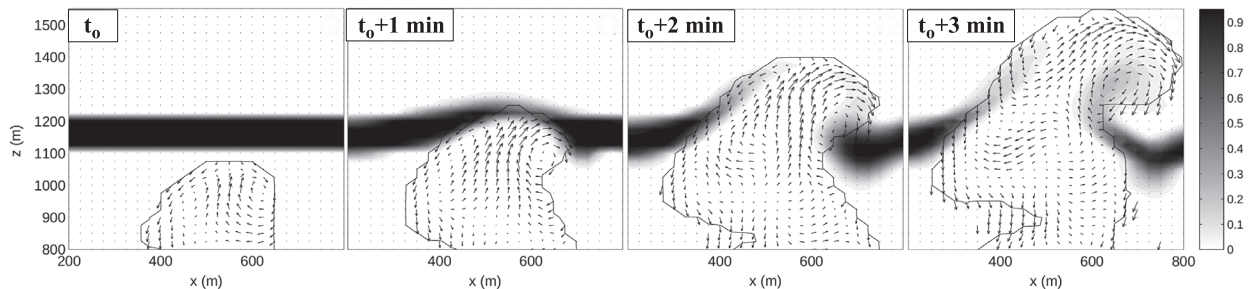

Fig. 13. Time sequence of four successive vertical cross-sections centred on the upper part of a growing cloud, with a 1-min frequency, starting t_o = 7.5 min after the initiation of the cloud. Arrows indicate wind in the cross-section. The contour delineates the cloud, defined as the area where the liquid water mixing ratio r_c is lower than 0.01 g kg^{-1}. The shading indicates the mixing ratio of a tracer r_t introduced at the time of the first snapshot uniformly in a layer extending from 1100 to 1200 m at a 1 g kg^{-1} concentration; Starting at $t = t_o$ + 1 min (b), the cloudy air penetrates and deforms this layer, and transports the tracers upwards, mainly on the edges of the cloud – adapted from Zhao and Austin (2005), © Copyright 2005 AMS.

with LES performed over ocean with increasing SST (Wyant et al., 1997; Sandu and Stevens, 2011). These studies generally support the major role of the SST, but also underline the significance of other factors such as the lower atmosphere lapse rate, or the magnitude of large-scale divergence, to precisely explain the characteristics of observed transitions.

Driven by this same aim to better understand cloud structures and processes, more and more, passive or Lagrangian tracers are introduced in LES and CRMs to track the circulation of air in relation to the clouds and to better depict the associated transport. As an example, Zhao and Austin (2005) used passive tracers to analyse the life cycle of simulated trade-wind cumulus clouds, each a few hundreds of metres deep and lasting less than half an hour. A first tracer was introduced in the sub-cloud layer

in order to better define the neighbouring area affected by the transport from the cloud, and they showed that it corresponds to roughly two to three times the cloud area as identified by liquid water content. A second tracer was introduced in an upper layer (Fig. 13) to analyse the mixing dynamics of each cloud. In particular, they showed that the mixing was mainly produced by the turbulent motions at the ascending cloud top, characterized by a complex vortical circulation with a strong ascending branch in the centre of the clouds, a large divergence at the top and subsidence at the edges, consistent with laboratory results of ascending thermals. Heus et al. (2008) used Lagrangian tracers to explore exchanges of air between cumulus clouds and their close environment. They focused on the narrow subsiding shells developing on their lateral sides (Jonas, 1990) and

identified evaporative cooling as a major driver of this cloud-interface dynamic structure (see also Park et al., 2017). They further suggested that the associated downward mass flux largely balances the upward mass flux occurring inside the cumulus, i.e. a view that departs from current conceptual schemes of the vertical motions arising in the environment of convective clouds – these assume that the mass balance is realized uniformly on a wider area (Jonker et al., 2008).

Considering now deep convective phenomena, LES are also well suited to address the increasing focus on their non-stationary transition phases (e.g. within the diurnal cycle over land) and more broadly, on the mechanisms accounting for the life cycle of transient deep convective systems, notably those arising at mesoscale. For instance, even though the interactions between the convective boundary layer and deep convection have been emphasized for a very long time (Ludlam, 1966), it is only now that this issue can be addressed numerically with a resolution fine-enough to explicitly simulate boundary-layer thermals and a domain size that is large enough to contain deep convective cells or mesoscale convective systems. Huang et al. (2009) showed using LES that the initiation of deep convection was favoured when boundary-layer thermals organized into open cells compared to rolls and they relate this sensitivity to differences in the vertical velocities and water vapour contents of thermals. The LES study of Böing et al. (2012), which analyses deep moist convection over a tropical homogeneous land surface, suggests that deep clouds differ mainly from shallow clouds by their size at cloud base rather than by their thermodynamic properties at that height. This complements the results of Khairoutdinov and Randall (2006), who found with another LES of this same case study that the rapid growth of deep convection was related to boundary-layer heterogeneities created by the evaporation of rainfall.

More generally, observations (Barnes and Garstang, 1982; Zuidema et al., 2012; Dione et al., 2014; de Szoeke et al., 2017) and such simulations both point to the importance of convectively-generated cold pools which are illustrated in Fig. 14. It emphasizes the coupled fluctuations of temperature, vertical velocity and wind speed characterizing this phenomenon. In particular, as the cold pools spread into the boundary layer, they generate narrow updraught at the front of the cold pools, and thus provide an efficient mechanical lifting for initiating new deep cells. Note also the very strong enhancement of wind speed, which, over ocean, can substantially increase surface heat and momentum fluxes (Redelsperger et al., 2000b), and over arid land accounts for large uplift of mineral dust (Takemi, 2005; Marsham et al., 2011). The basic physics behind the dynamics of such cold pools is relatively well understood. However, their interactions with the boundary-layer dynamics (e.g. how strong BL thermals affect their sharp boundaries and strength) and with surface processes, the precise mechanisms through which they help sustain further convection (e.g. mechanical lifting vs. modification of the thermodynamics), are

still poorly known (see for instance the contrasting findings of Tompkins (2001) and Zuidema et al. (2012)). These questions are just starting to be addressed with LES which are now able to provide realistic depictions of such transient sequences (e.g. Böing et al., 2012; Seifert and Heus, 2013; Schlemmer and Hohenegger, 2014; Torri et al. 2015), and their representation in large-scale models is in its infancy; to date, a parametrization of cold pools has been implemented in one single large-scale model (Hourdin et al., 2013; Grandpeix and Lafore, 2010).

At larger scale also, a few CRMs or convective-permitting simulations have been used to study phenomena, such as the intraseasonal Madden–Julian Oscillation (MJO) or the monsoon systems. This include simulations performed over wide regional-scale domains (Holloway et al., 2013; Marsham et al., 2013; Birch et al., 2014) or over the whole globe (using either the
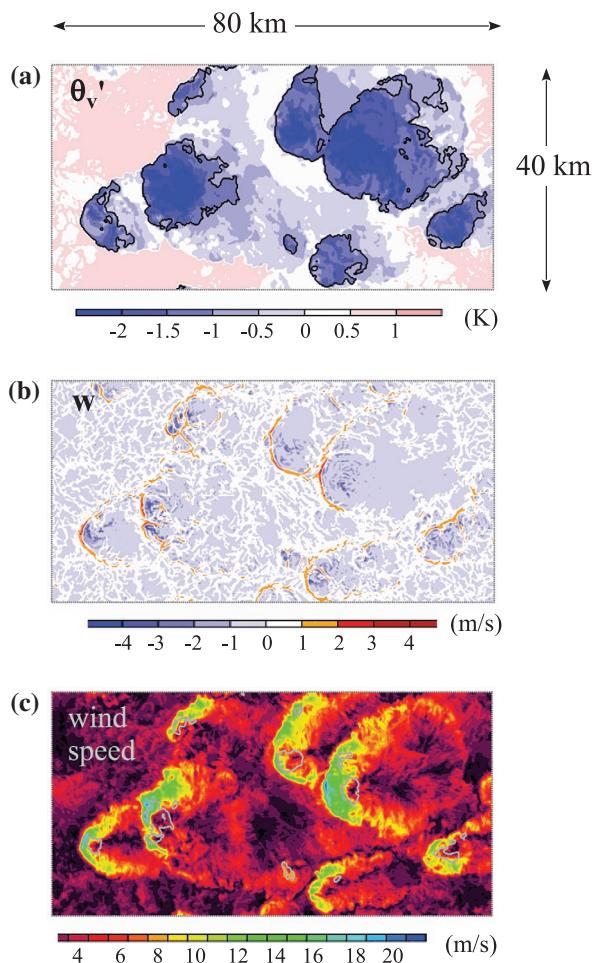

Fig. 14. Horizontal cross-section of potential temperature anomaly (a), vertical velocity (b) and wind speed (c) close to the surface, from a LES of deep convection over land. The figures illustrate the properties of the convectively generated cold pools: pools of negative temperature anomalies (a) with strong upward motion at their front – narrow orange stripes in (b) – and horizontal wind gusts – green and blue zones in (c).

super-parametrization framework (Grabowski, 2003) or global models using a few km wide grid mesh (Tomita et al., 2005)) – note that such simulations require substantial computing power too. The MJO is not well explained by classical theories and its simulation with conventional large-scale weather and climate models is difficult and highly sensitive to physical parametrizations (Zhang, 2005; Lin et al., 2006; Bechtold et al., 2008; Del Genio et al., 2015). By contrast, it appears that convection-permitting simulations are more successful to reproduce this major tropical intraseasonal fluctuation (Graboswki, 2003; Khairoutdinov et al., 2005; Miura et al., 2007; Thayer-Calder and Randall, 2009; Holloway et al., 2013). These studies underline the importance of convective processes in moistening the free troposphere; they also highlight a positive feedback between water vapour and moist convection, whereby moist convection generates large-scale water vapour heterogeneities which further affect the spatial structure of deep convection at that scale (in such a way that these large-scale convective organizations disappear when the water vapour heterogeneities are artificially damped).

5.3. LES and CRMs as guidance for parametrizations of convective and cloud-related processes

Numerous studies have shown that it is important to design more physically-based convective and cloud parametrizations in order to improve the performances of large-scale models. LES and CRMs can be used on their own to test hypotheses used in the parametrizations. Several studies have analysed LES and CRMs from this perspective as briefly illustrated below.

Here, it is useful to recall that nowadays, most convective parametrizations are built on a formulation of convective mass fluxes based on simplified sets of equations (Arakawa and Schubert, 1974; Tiedtke, 1989). They generally involve (i) the determination of convective mass fluxes at cloud base (referred to as the "parametrization closure"[9]), (ii) the estimation of lateral entrainment and detrainment rates which control the mass and water exchanges of convective elements with their environment and dictate the vertical shape of convective mass fluxes and (iii) the definition of triggering criteria for the activation of the convective parametrization. A few CRM studies have analysed the relevance and limitations of the mass-flux formulation, for instance, the use of generic "bulk" convective droughts as in Tiedtke (1989) to represent an ensemble of convective clouds, the assumption of a steady-state of this ensemble, or the links between the actual in-cloud entrainment and the lateral entrainment models used in convective parametrizations (e.g. Gregory and Miller, 1989; Xu, 1995; Guichard et al., 1997; Lin and Arakawa, 1997; Yano et al., 2004; Romps, 2010). Several other studies have directly focussed on the sensitivity of this lateral entrainment to large-scale (in the sense of resolved) variables, on its magnitude and fluctuations with height (Siebesma and Holtslag, 1996; Romps and Kuang, 2010 – see

also de Rooy et al. (2013) for a review). Most LES and CRM analyses of the mechanisms responsible for the development, or triggering, of deep convection are relatively recent (Redelsperger et al., 2002; Chaboureau et al., 2004; Khairoutdinov and Randall, 2006; Böing et al., 2012; Couvreux et al., 2015; Rochetin et al., 2014). An obvious cause is that as soon as boundary-layer processes are involved, the explicit simulation of both boundary layer and deep cloud motions requires a fine grid mesh over large domains. For similar reasons, in the past, CRM studies of convective parametrization closures have been few (e.g. Xu, 1994; Cohen and Craig, 2004), because the closure problem involves interactions of deep convection with its larger-scale environment, so that only limited insight could be gained at that time with CRM. As computing resources increases, it seems very likely that several of these parametrization-related issues will be revisited.

In the last few decades, the approach to the development and improvement of the convection and cloud parametrizations used in large-scale weather and climate models has changed considerably. Nowadays, it often involves several steps, where LES and CRMs play an increasingly important role. This includes (i) joint-analyses of observations and high-resolution simulations (LES or CRM) in order to explore and study the processes to be parametrized, and to define and analyse relevant parametrization-oriented diagnostics, (ii) the development of the parametrization itself, (iii) a first phase of assessment of the parametrization with the SCM version of the large-scale model, typically involving extensive process-oriented comparisons with LES or CRM simulations and evaluation of the improvements and (iv) an evaluation and validation within the 3D large-scale model.

Initial and boundary conditions used in LES and CRM simulations can often be very similarly applied to SCM, and this allows a *direct* comparison between both types of simulations (Randall et al., 1996). The joint utilization of LES and SCM is now part of a common methodology that was advocated by the GEWEX (Global Energy and Water Cycle Experiment) Cloud System Study (GCSS) project (Browning and The GEWEX Cloud System Science Team, 1993) for the development of convective and cloud parametrizations (Siebesma and Holtslag, 1996; Hourdin et al., 2013). Three major interests of SCM simulations are (i) their very low numerical cost compared to full 3D simulations and (ii) their particular setup which prevents feedbacks between the large-scale dynamics and the parametrizations, thus leading to easier, more straightforward interpretations, (iii) the possibility to assess the functioning of parametrizations in realistic conditions.

LES and CRMs can efficiently serve as a bridge between complex observations and the more crude SCMs. Indeed, they provide explicit simulations of convective motions and clouds that can be compared to – and evaluated with – observations acquired at the same scale. It can then be valuable to simplify the setup of such simulations to address specific questions or to

study some mechanisms in more detail (Krueger et al., 2016). LES and CRM simulations correspond then to the references against which SCM are evaluated. A first-order evaluation generally consists in comparing the simulated mean profiles of temperature, water vapour and clouds obtained with both types of models (e.g. Hourdin et al., 2002; Lenderink et al., 2004; Guichard et al., 2004; Siebesma et al., 2007; Rio and Hourdin, 2008; Neggers, 2009; Pergaud et al., 2009). It is also valuable to assess the contribution of convective processes to the heat and water budget, and to their combination in the moist static energy budget.

LES or CRMs can further be used to derive parametrization-oriented information, corresponding to diagnostics of those variables that are internal to the parametrizations such as the vertical structure of convective mass fluxes and their partition between convective and stratiform parts of mesoscale convective systems (Gregory and Guichard, 2002), or the estimation of entrainment and detrainment rates in clouds (Siebesma and Holtslag, 1996; Gregory, 2001). Analysing a LES of shallow cumulus clouds, Siebesma and Holtslag (1996) were the first to point to unrealistic formulations of entrainment and detrainment in parametrizations, with too low values of both, and to propose revised formulations that accounted for the decreasing convective mass flux from the bottom to the cloud top (Fig. 15). The vertical profiles of entrainment and detrainment from the surface to the cloud tops were analysed in more detail by Couvreux et al. (2010) using passive tracers to track the air forming boundary-layer thermals, and this analysis was further used to define and calibrate new formulations of parametrized convective entrainment and detrainment rates accounting for both the subcloud and the cloud layers (Rio et al., 2010). Numerous other diagnostics, such as the vertical velocity budget (de Roode et al., 2012) or the joint probability functions of vertical velocity and conserved variables, as well as multivariate distributions of hydrometeors (Larson et al., 2002; Jam et al., 2013; Griffin and Larson, 2016) have been used to guide the development of convection and cloud parametrizations.

LES and CRMs will probably remain important tools for these developments in the future, for the calibration of parameters (e.g. entrainment coefficients, convective drought properties), but also (i) to help renew some of the basic assumptions made in convective parametrizations and (ii) to advance on the parametrization of the interactions of convective processes with other physical processes such as boundary-layer turbulence, microphysics, radiative and surface processes.

5.4. Exploration of basic climatic issues

Cloud and precipitation climatic sensitivities are most often analysed and interpreted from coarse-grid climate models (Bony et al., 2006; Brient and Bony, 2013). However, climate models are notoriously sensitive to convective and cloud parametrizations (Hourdin et al., 2006; Neggers, 2015 among many), for instance
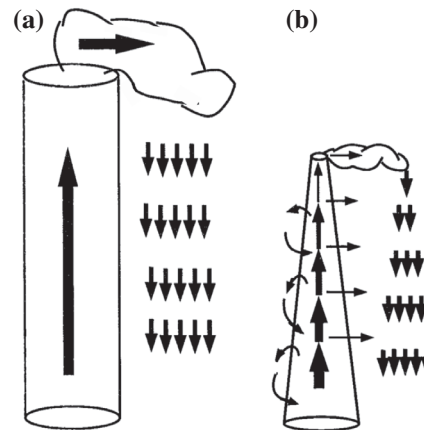

Fig. 15. Comparison of conceptual schemes of turbulent mixing in parametrized shallow cumulus clouds when using either (a) weak and equal values of entrainment and detrainment rates ε and δ, or (b) stronger values of both with $\Delta > \varepsilon$, as suggested by LES. The length and width of the arrows indicate the strength of mass fluxes. In (a), there is hardly any horizontal exchange between cloud air (within the cylinder) and its surrounding up to cloud top where detrainment is then massive, while in (b), the enhanced lateral mixing and the fact that detrainment dominates over entrainment over the whole cloud depth leads to a decrease of the convective mass flux with height (represented by a cone shape) and to much less detrainment at cloud top – adapted from Siebesma and Holtslag (1996), © Copyright 1996 AMS.

entrainment and microphysical processes, such as ice fall speed (Sanderson et al., 2008) – note that this is not exclusive of sensitivities to other aspects of those parametrizations. This sensitivity can affect the simulated climate in different ways, via changes in the global-mean climate, or in the geographic location of major regional features, such as the inter-tropical convergence zone (Oueslati and Bellon, 2013), or, at smaller space and time scales, via changes in the intensity of precipitation (Wang et al., 2016). Furthermore, there is currently a wide spread among those models, in terms of climate and climatic sensitivity to clouds (Vial et al., 2013; Ceppi et al., 2017). Therefore, studies of convective and cloud climatic feedbacks based on climate model results are informative of the functioning of models, but the limitations mentioned above preclude drawing firm conclusions about the relevance of these feedbacks.

From another perspective, and beyond their utilization for process-type studies (Section 5.2) and convective parametrizations (Section 5.3), LES and CRMs can also be used to explore climatic issues, i.e. climatic feedbacks associated with convection and clouds. Here, these fine-scale models are generally not considered as a substitute for full GCM. Rather, they are used for gaining complementary insights into these questions. For instance, one can study the impact of idealized climate change perturbations such as a change in SST or an increase in atmospheric CO_2 on the cloud cover (does it increase or decrease? and via which mechanism?), on the hydrological cycle (does

it rain more or less? does the intensity of rainfall change? and if so, at which scale?). A major interest of this approach is also the possibility to explore the sensitivities of the results to the couplings between physical processes in a comprehensive way.

An archetypal example of an academic concept (or frame) which can potentially help address basic climatic issues is the radiative–convective equilibrium (RCE). The RCE connects surface temperature to radiative forcing at large scale with very simplified models of the Earth system, an approach pioneered by Manabe and Wetherald (1967) The RCE frame has since been revisited many times. In its simple form it consists of a single-column atmospheric model which incorporates a formulation of convective and radiative processes (plus some assumptions at the surface; e.g. a prescribed albedo), and simulations are run until a thermodynamic equilibrium is reached. By design, the RCE concept is more directly relevant to global climate issues, and notably departs from reality where the large-scale context fluctuates from day to day (e.g. synoptic changes associated with tropical waves), and the convective adjustment time scale varies with this context. Therefore, there is no simple nor direct connection between results from such 1D simulations, the 3D climate simulations performed with the same parametrizations (Brient and Bony, 2012) and the more complex and varied situations observed in the real world (Cohen and Craig, 2004; Keil et al., 2014).

Keeping these limitations in mind, this type of idealized simulation can be carried out with a CRM instead of a single-column model, and this was indeed first experimented in the 90s (Sui et al., 1994; Tompkins and Craig, 1998; Xu and Randall, 1999; Muller et al., 2011; Tompkins and Semie, 2017). Typically, these simulations use periodic boundary conditions together with a prescribed SST. The time required to reach a thermodynamic equilibrium, driven by radiative processes, is typically on the order of 10 days. One must remember that, even though the interactions among processes are represented in a more explicit way than in fully parametrized models, the content of physical parametrizations has more time to imprint the results than in shorter duration runs. For instance, over ocean, radiative processes can only weakly affect the mean temperature profile in one-day runs, but their contribution becomes much more important when focussing on multi-day time scales (Guichard et al., 2000). Indeed, Tao et al. (1999) found that differences in the formulation of surface heat flux largely accounted for the very contrasted temperature and water vapour at equilibrium obtained with two CRMs. Tompkins and Semie (2017) also showed that the ability of deep convection to organize into mesoscale systems is sensitive to the turbulent and diffusion schemes, via their impact on the entrainment mixing in convective updraught. It seems likely that the choice of the microphysical scheme would also affect the results, especially for simulations coupled to an upper ocean layer. However, this framework can still be quite insightful. Fig. 16a (from Tompkins and Craig, 1998) shows the spatial structure of convection in

such a RCE simulation where the mean wind and wind shear were weak. However, convection displays mesoscale banded structures which turn out to emerge from interactions between surface fluxes, atmospheric radiation and convective processes (compare with Fig. 16b and c). In particular, taking into account convective-radiative interactions leads to more convergence in the cloudy areas and longer lasting clouds. Sensitivities of convective spatial patterns to the wind field (which are generally neglected in parametrizations of convection) can be even more spectacular (Muller, 2013 and Fig. 17), and are accompanied by changes in the cloud cover, water and energy budgets.

More recently, the WTG framework, distinct from the CRE framework in the formulation of its boundary conditions (cf Section 4.5), was also used in CRMs to investigate climatic issues (in a RCE mode). A peculiar result arising from these studies is the existence of multiple equilibria for a given SST, with a final equilibrium, either dry vs. wet, largely controlled by the initial water vapour field (Sessions et al., 2010; Daleu et al., 2015). Ruppert (2016) also used the WTG framework to analyse the role of the diurnal cycle of radiation on convection and clouds. This short time-scale fluctuation is often neglected in RCE but his results emphasize their profound impact on the mean simulated climatic state, with the development of deeper and more active convective clouds via mechanisms involving the radiative budget and static stability. Whether these findings are fully relevant to tropical convective activity is an open issue which needs further elaboration, but they renew the current static view of the tropical radiative-convective equilibrium.

The projected climatic increase in the intensity of rain events with warming (Emori and Brown, 2005; O'Gorman, 2015; Westra et al., 2014) together with observational studies emphasizing an intensification of heavy-rain events in the last decades (Lenderink and Van Meijgaard, 2008; Panthou et al., 2014; Taylor et al., 2017 among many) also motivated a few recent CRM-based studies. It must be noted here that extreme precipitation events are not simply constrained by the Clausius–Clapeyron (CC) scaling (which indicates a ~ 7% in water vapour amount increase per K). Their sensitivity to warming also involves changes in the dynamics and in the microphysics (O'Gorman, 2015). Muller et al. (2011) used budget equations of RCE CRMs differing in their SST to explore the causes behind the increase of the higher percentiles of precipitation with warming. They could infer that the thermodynamic constraint was dominating the response of precipitation extremes in their case, despite stronger convective updraught velocities. Romps (2011) reached the same conclusion albeit using a smaller domain and a finer grid mesh. However, he also found a positive contribution of the convective dynamics. Finally, Singh and O'Gorman (2014) further emphasized the sensitivity of precipitation extremes to the representation of hydrometeor fall speeds. It is possible that the change in extreme rainfall intensity were constrained by the use of periodic condition in these studies. Indeed, Singleton and Toumi (2013) analysed the
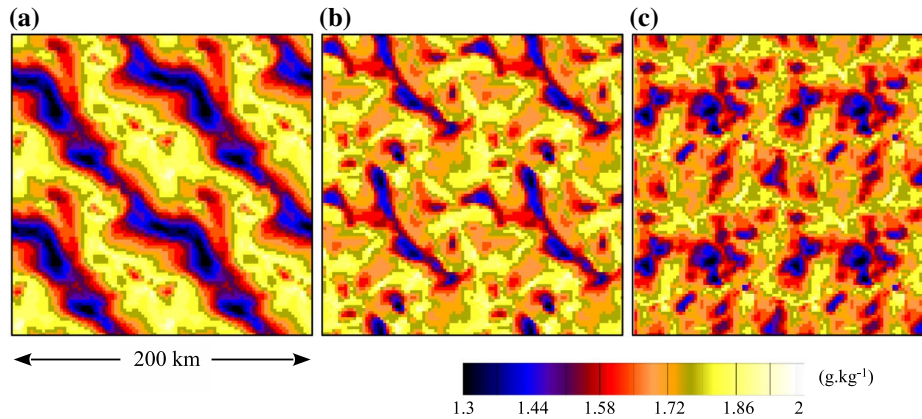
Fig. 16. An illustration of the sensitivity of the spatial structure (or organization) of deep tropical convection to the coupling with physical processes in convective radiative equilibrium (CRE) simulations. The plots show the water vapour mixing ratio at the lowest model level for (a) a reference simulation, (b) a simulation where surface fluxes do not respond to mesoscale fluctuations of the surface wind and (c) a simulation where radiative processes are prescribed instead of computed from the thermodynamical profiles and cloud field. The domain is replicated four times so that each panel represents a 200 km × 200 km square – adapted from Tompkins and Craig (1998), © Copyright 1998 RMS.
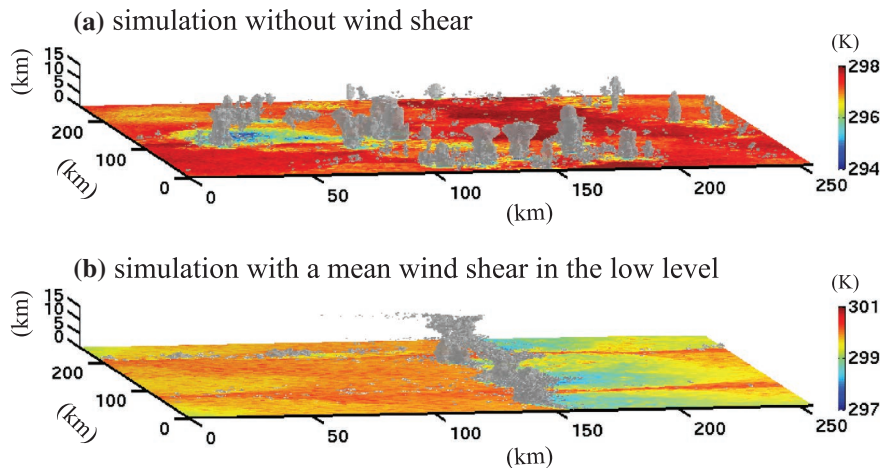

Fig. 17. Snapshots of clouds (grey volumes) and near-surface air temperature (shading) in two convective–radiative equilibrium CRM runs, one without wind shear (a) and the other with shear in the lower atmosphere (b). The presence of shear changes the spatial scale of convective patterns, with isolated cells replaced by squall-line-type systems – adapted from Muller (2013), © Copyright 2013 AMS.

sensitivity of a squall-line to an increase of the atmospheric temperature with a CRM using partly open boundary conditions and found a much stronger increase of precipitation with a system-mean rainfall scaling at 1.5 CC.

Bretherton et al. (2013) also examined climate change sensitivities in three different regimes of subtropical cloudy boundary layers, well-mixed stratocumulus, cumulus beneath stratocumulus and cumulus, with the aim to help interpretation of climatic projection. In practice this was done by perturbing the setup of the LES in ways consistent with large-scale climate change expectations. This included modifications of temperature, CO_2 concentration, subsidence, relative humidity and wind speed. For the two first regimes, they found a positive

cloud feedback, with a reduction of the shortwave cloud radiative effect (mainly due to cloud thinning). This positive feedback was explained by dominating effects of atmospheric warming and moistening with increased CO_2 against the impact of the weaker subsidence that induced a deepening of the cloud layer. No such cloud-radiation feedback was identified in the cumulus regime. This cloud feedback analysis is further supported by a LES intercomparison of these cases (Blossey et al., 2013), and contrasts with the spread in the results obtained with SCMs (Zhang et al., 2013). The LES results of Vogel et al. (2016) similarly point to a small climatic feedback of shallow cumulus. The authors also underlined the major importance of the large-scale horizontal advection, which is prescribed in such

LES of boundary-layer cloud feedbacks, because it strongly affects the simulated structure of the lower atmosphere.

The idealized simulations discussed in this section contribute to advancing our general understanding of convection and cloud climatic sensitivities. They generally emphasize that the climatic sensitivity of both shallow and deep convective clouds arises from delicate balances involving compensating mechanisms between physical processes. Their links with the climate sensitivity of the real world are not straightforward though. In particular, they do not properly account for feedbacks between convective processes and larger-scale circulations. However, despite these limitations, they allow exploring in a simple way physically-based mechanisms of interactions and feedbacks that are not well accounted for in current climate models (e.g. mesoscale organization and its impact on the mean climatic state, causes of changes in extreme precipitation or shallow cloud climatic sensitivity). Furthermore, as discussed in the following section, new emerging approaches using convection-permitting modelling over region-wide domains will allow to more fully explore numerous climatic issues involving moist convection that can only be partly addressed with idealized simulations (e.g. Kendon et al., 2014; Meredith et al., 2015).

6. Conclusion and perspectives

As extensively discussed above, LES and CRMs are fine-scale limited-area numerical models whose major characteristic is to provide explicit simulations of the mesoscale dynamics associated with convective clouds. They integrate parametrizations in order to represent major sub-grid processes (turbulence, microphysics, radiative processes). However, unlike GCMs, their grid size allows numerous couplings arising between convective motions and physical processes to be resolved. It took several decades to develop these models to the point where they stand now, comprising numerous phases of evaluation, refinement and improvement. In the meantime, their utilization has proved very fruitful to the understanding of several convective cloud-related issues that cannot be satisfactorily addressed with observations alone; they are also now widely used as 'numerical laboratories' which guide and help the development of cloud and convection parametrizations for larger-scale models. In the past, this often involved using one or two particular case studies prior to the implementation of new or modified parametrizations in 3D large-scale models. As new LES and CRM simulations become available over a variety of convective regimes and climatic areas, we think that it would be useful to introduce an intermediate step that would consist in a systematic assessment of the parametrizations over all case studies prior to the implementation in the 3D model. The calibration of climate models is a major issue (Hourdin et al., 2016). Currently, it is mostly realized at the global scale, which can hide a number of compensating errors. The use of this

ensemble of LES and CRMs simulations for tuning the SCM versions of climate models could be an integral part of this intermediate step. It would constitute a new, more physically-based methodology for the tuning of climate model.

It would be misleading to consider LES and CRM as frozen models. Firstly, whenever using such a model, it is necessary to be aware of its formulation, of the thermodynamics and boundary conditions in particular, of its parametrizations of physical processes and of their couplings. Secondly, a large amount of work is still dedicated to the improvement of these models, of their parametrizations and numerics in particular. Additional model developments are also necessary to explore a range of scientific issues; small-scale couplings between turbulence and microphysics, couplings with land-surface or ocean mixed-layer models, mesoscale topography, introduction of dust surface uplift, aerosol, chemistry.

Still, it seems very likely that these fine-resolution models will remain very useful in the near future. As previously mentioned, most LES and CRM studies have focussed on convective clouds over ocean, but the relevance of their findings to moist convection developing over land is not obvious (because of major differences in environments and in the balances of processes). However, with some developments, these models are also well suited to address the numerous issues related to surface-atmosphere feedbacks over land (Trier et al., 2004; Schlemmer et al., 2011; Froidevaux et al., 2014; Rochetin et al., 2017). We speculate that they will be very useful to explore how surface fluxes and surface mesoscale heterogeneities influence the initiation, strength and life cycle of daytime convection, and to assess how the environment potentially modulates these feedbacks. At a larger scale, this should help to identify new modes of interactions between mesoscale and larger-scale circulations involving convection and clouds (e.g. synoptic-scale waves and intra-seasonal modes of variability) and to design parametrizations of these mesoscale process for coarse-resolution models.

Numerous perspectives also arise due to increasing computing power (even if it is not the solution to all problems). This allows performing simulations with either enhanced resolution and/or larger domain sizes and integration times. Recent progress has been achieved on this latter front (i) with LES carried out over an entire year over an observatory (Schalkwijk et al., 2015) or over very large domains (Seifert and Heus, 2013; Dauhut et al., 2015; Heinze et al., 2017) and (ii) convection-permitting regional simulations (typically grid size less than 5 km) carried out over wide regions for a few days to a few years, such as performed more and more frequently nowadays (Prein et al., 2015). Marsham et al. (2013) show with such simulations how the West African monsoon circulation is radically changed over West Africa (and improved in several ways) when deep convection is explicitly simulated. This result involves changes in the diurnal phasing of convection (typically better reproduced

in CRMs than parametrized models) and a contribution of the vertical mass flux associated with convectively-generated cold pools to atmospheric low-level cooling, i.e. a process which is distinct from the cooling otherwise operated at larger scale by the monsoon flow via horizontal advection. Over this same region, Taylor et al. (2017) identified a very sharp increase of the intensity of Sahelian MCS and heavy precipitating events in the last decades, but this increase appears unrelated to temperature (as locally, there was no warming trend). Rather, it appears to be linked to a climatic change of the wind shear over this region. Modelling studies using convection-permitting regional simulations are much better suited to analyse the influence of wind shear on MCS trends than climate models using convective parametrizations, as the latter generally ignore the influence of wind shear. More broadly, an important perspective for the future decade is to explore how the climate sensitivities of large-scale phenomena (e.g. monsoons, inter-tropical convergence zone) to moist convection depart – or not – from those simulated with large-scale models which parametrize moist convection. This includes long term mean climates and their regional contrasts as well as extremes, such as heavy rain events.

Finally, at even larger-scale, in the past decade, global simulations of a novel type, using the super-parametrization framework (Grabowski, 2001; Randall et al., 2003) have been very helpful to study climatic phenomena that are not well simulated by conventional global models using convective parametrizations. The pioneer development of a convection-permitting global model by Satoh et al. (2008) also demonstrated the value of high-resolution global simulations that could be performed without parametrizing deep convection. It is now followed by other initiatives (Skamarock et al., 2012). These models are conceptually simpler that global models using the super-parametrization framework, and their development is likely to continue in the next decades, even if they are more demanding in terms of computing power. By then, the utilization of CRM simulations performed over mesoscale-size domains may become rare. However, it seems likely that LES of clouds and convection will still constitute a central tool for the development of the physical parametrizations of these future models, and that they will also be incorporated in those models in the form of high-resolution nested models.

Acknowledgements

Disclosure statement

Funding

Notes

1. Note also that LES of convection have often been compared to laboratory analogues; e.g. with water tanks, but there are no straightforward analogues for cumulus convection.
2. In the sense that they deliberately depart from the real world by several aspects.
3. Where a 'smoke cloud' can be thought of as a cloud which is radiatively active, but where no water phase or microphysical processes change take place.
4. Note however, that a more general distribution function, expressed as $n(D) = n_0 D^\alpha\ e^{-\lambda D}$, a Gamma function, is often considered for solid hydrometeors, following Ulbrich (1983).
5. The same applies to simulations of the dry convective boundary layer.
6. The single scattering albedo ω is the ratio of scattering to extinction (sum of scattering and absorption); ω ranges from 1 for purely scattering particles to 0 when extinction is solely due to absorption. For clouds, it is typically well above 0.5.
7. The asymmetry factor is an indicator of the direction of scattering with $g = -1$ ($g = 1$) for backward (forward) scattering.
8. The effective radius r_e is the ratio of the third to the second moment of the particle size distribution. In the case of (non-spherical) ice particles, r_e is estimated using spheres of equal surface area.
9. A common approach for the closure of convective parametrization consists in relating the cloud-base mass flux to the large-scale convective available potential energy (CAPE) – see Yano et al. (2013) for a review of existing closures.

References

Abma, D., Heus, T. and Mellado, J. P. 2013. Direct numerical simulation of evaporative cooling at the lateral boundary of shallow cumulus clouds. *J. Atmos. Sci.* **70**, 2088–2102.

Albrecht, B. A., Bretherton, C. S., Johnson, D., Scubert, W. H. and Frisch, A. S. 1995. The Atlantic Stratocumulus Transition Experiment – ASTEX. *Bull. Amer. Meteorol. Soc.* **76**, 889–904.

Arakawa, A. and Schubert, W. H. 1974. Interaction of a cumulus cloud ensemble with the large-scale environment, Part I. *J. Atmos. Sci.* **31**, 674–701.

Arakawa, A. and Konor, C. S. 2009. Unification of the anelastic and quasi-hydrostatic systems of equations. *Mon. Wea. Rev.* **137**, 710–726.

Asa, T. and Nakamura, K. 1978. A numerical experiment of airmass transformation processes over warmer sea. Part I: Development of a convectively mixed layer. *J. Meteorol. Soc. Japan* **56**, 424–434.

Atkinson, B. W. and Zhang, J. W. 1996. Mesoscale shallow convection in the atmosphere. *Rev. Geophys.* **34**, 403–431.

Baba, Y. and Takahashi, K. 2013. Weighted essentially non-oscillatory scheme for cloud edge problem. *Q.J.R. Meteorol. Soc.* **139**, 1374–1388.

Bannon, P. R. 1996. On the anelastic approximation for a compressible atmosphere. *J. Atmos. Sci.* **53**, 3618–3628.

Barnes, G. M. and Garstang, M. 1982. Subcloud layer energetics of precipitating convection. *Mon. Wea. Rev.* **110**, 102–117.

Basu, S. and Porté-Agel, F. 2006. Large-eddy simulation of stably stratified atmospheric boundary layer turbulence: a scale-dependent dynamic modeling approach. *J. Atmos. Sci.* **63**, 2074–2091.

Bechtold, P., Köhler, M., Jung, T., Doblas-Reyes, F., Leutbecher, M. and co-authors. 2008. Advances in simulating atmospheric variability with the ECMWF model: from synoptic to decadal time-scales. *Q.J.R. Meteorol. Soc.* **134**, 1337–1351.

Birch, C. E., Parker, D. J., Marsham, J. H., Copsey, D. and Garcia-Carreras, L. 2014. A seamless assessment of the role of convection in the water cycle of the West African Monsoon. *J. Geophys. Res.* **119**, 2890–2912.

Blossey, P. N., Bretherton, C. S., Zhang, M., Cheng, A., Endo, S. and co-authors. 2013. Marine low cloud sensitivity to an idealized climate change: The CGILS LES intercomparison. *J. Adv. Model. Earth Syst.* **5**, 234–258.

Bogenschutz, P. A., Krueger, S. K. and Khairoutdinov, M. 2010. Assumed probability density functions for shallow and deep convection. *J. Adv. Model. Earth Syst.* **2**, 10.

Böing, S. J., Jonker, H. J., Siebesma, A. P. and Grabowski, W. W. 2012. Influence of the subcloud layer on the development of a deep convective ensemble. *J. Atmos. Sci.* **69**, 2682–2698.

Bony, S., Colman, R., Kattsov, V. M., Allan, R. P., Bretherton, C. S. and co-authors. 2006. How well do we understand and evaluate climate change feedback processes? *J. Climate.* **19**, 3445–3482.

Bougeault, P. 1981. Modeling the trade-wind cumulus boundary layer. Part I: Testing the ensemble cloud relations against numerical data. *J. Atmos. Sci.* **38**, 2414–2428.

Bougeault, P. and Lacarrere, P. 1989. Parameterization of orography-induced turbulence in a mesobeta–scale model. *Mon. Wea. Rev.* **117**, 1872–1890.

Bretherton, C. S., Blossey, P. N. and Jones, C. R. 2013. Mechanisms of marine low cloud sensitivity to idealized climate perturbations: A single-LES exploration extending the CGILS cases. *J. Adv. Model. Earth Syst.* **5**, 316–337.

Brient, F. and Bony, S. 2012. How may low-cloud radiative properties simulated in the current climate influence low-cloud feedbacks under global warming? *Geophys. Res. Lett.* **39**, L20807.

Brient, F. and Bony, S. 2013. Interpretation of the positive low-cloud feedback predicted by a climate model under global warming. *Clim. Dyn.* **40**, 2415–2431.

Brown, A. R., Cederwall, R. T., Chlond, A., Duynkerke, P. G. and co-authors. 2002. Large-eddy simulation of the diurnal cycle of shallow cumulus convection over land. *Q.J.R. Meteorol. Soc.* **128**, 1075–1093.

Brown, P. R. A. and Swann, H. A. 1997. Evaluation of key microphysical parameters in three-dimensional cloud-model simulations using aircraft and multiparameter radar data. *Q.J.R. Meteorol. Soc.* **123**, 2245–2275.

Browning, K. and The GEWEX Cloud System Science Team. 1993. The GEWEX cloud system study (GCSS). *Bull. Amer. Meteorol. Soc.* **74**, 387–399.

Brümmer, B. 1999. Roll and cell convection in wintertime arctic cold-air outbreaks. *J. Atmos. Sci.* **56**, 2613–2636.

Bryan, G. H., Wyngaard, J. C. and Fritsch, J. M. 2003. Resolution requirements for the simulation of deep moist convection. *Mon. Wea. Rev.* **131**, 2394–2416.

Carpenter, K. M. 1982. Note on the paper 'Radiation conditions for lateral boundaries of limited area numerical models'. *Q.J.R. Meteorol. Soc.* **108**, 717–719.

Ceppi, P., Brient, F., Zelinka, M. D. and Hartmann, D. L. 2017. Cloud feedback mechanisms and their representation in global climate models. *WIREs Clim. Change* **8**, e465.

Chaboureau, J.-P., Guichard, F., Redelsperger, J.-L. and Lafore, J.-P. 2004. The role of stability and moisture in the diurnal cycle of convection over land. *Q.J.R. Meteorol. Soc.* **130**, 3105–3117.

Clark, T. L. 1977. A small-scale dynamic model using a terrain-following coordinate transformation. *J. Comput. Phys.* **24**, 186–215.

Clark, T. L., Hauf, T. and Kuettner, J. P. 1986. Convectively forced internal gravity waves: Results from two-dimensional numerical experiments. *Q.J.R. Meteorol. Soc.* **112**, 899–925.

Chung, D. and Matheou, G. 2014. Large-eddy simulation of stratified turbulence. part i: a vortex-based subgrid-scale model. *J. Atmos. Sci.* **71**, 1863–1879.

Cohen, B. G. and Craig, G. C. 2004. The response time of a convective cloud ensemble to a change in forcing. *Q.J.R. Meteorol. Soc.* **130**, 933–944.

Corbetta, G., Orlandi, E., Heus, T., Neggers, R. and Crewell, S. 2015. Overlap statistics of shallow boundary layer clouds: Comparing ground-based observations with large-eddy simulations. *Geophys. Res. Lett.* **42**, 8185–8191.

Cotton, W. R., Bryan, G. and Van den Heever, S. C. 2010. *Storm and Cloud Dynamics*. 2nd ed., Vol. 99. Academic Press, New York, NY.

Couvreux, F., Guichard, F., Masson, V. and Redelsperger, J. L. 2007. Negative water vapour skewness and dry tongues in the convective boundary layer: observations and large-eddy simulation budget analysis. *Bound-Layer Meteorol.* **123**, 269–294.

Couvreux, F., Hourdin, F. and Rio, C. 2010. Resolved versus parametrized boundary-layer plumes. Part I: A parametrization-oriented conditional sampling in large-eddy simulations. *Bound-Layer Meteorol.* **134**, 441–458.

Couvreux, F., Roehrig, R., Rio, C., Lefebvre, M.-P., Caian, M. and co-authors. 2015. Representation of daytime moist convection over the semi-arid Tropics by parametrizations used in climate and meteorological models. *Q.J.R. Meteorol. Soc.* **141**, 2220–2236.

Daleu, C. L., Plant, R. S., Woolnough, S. J., Sessions, S., Herman, M. J. and co-authors. 2015. Intercomparison of methods of coupling between convection and large-scale circulation: 1. Comparison over uniform surface conditions. *J. Adv. Model. Earth Syst.* **7**, 1576–1601.

Dauhut, T., Chaboureau, J.-P., Escobar, J. and Mascart, P. 2015. Large-eddy simulations of Hector the convector making the stratosphere wetter. *Atmos. Sci. Lett.* **16**, 135–140.

Deardorff, J. W. 1970. A three-dimensional numerical investigation of the idealized planetary boundary layer. *Geophys. Fluid Dyn.* **1**, 377–410.

Deardorff, J. W. 1972. Parameterization of the planetary boundary layer for use in general circulation models. *Mon. Wea. Rev.* **100**, 93–106.

Deardorff, J. W. 1980. Stratocumulus-capped mixed layers derived from a three-dimensional model. *Bound-Layer Meteorol.* **18**, 495–527.

Del Genio, A. D., Wu, J., Wolf, A. B., Chen, Y., Yao, M. S. and co-authors. 2015. Constraints on cumulus parameterization from simulations of observed MJO events. *J. Climate* **28**, 6419–6442.

de Rooy, W. C., Bechtold, P., Fröhlich, K., Hohenegger, C., Jonker, H. and co-authors. 2013. Entrainment and detrainment in cumulus convection: an overview. *Q.J.R. Meteorol. Soc.* **139**, 1–19.

de Roode, S. R., Siebesma, A. P., Jonker, H. J. J. and de Voogd, Y. 2012. Parameterization of the vertical velocity equation for shallow cumulus clouds. *Mon. Weather Rev.* **140**, 2424–2436.

de Roode, S. R., Sandu, I., van der Dussen, J. J., Ackerman, A. S., Blossey, P. and co-authors. 2016. Large-eddy simulations of EUCLIPSE–GASS Lagrangian stratocumulus-to-cumulus transitions: mean state, turbulence, and decoupling. *J. Atmos. Sci.* **73**, 2485–2508.

de Szoeke, S. P., Skyllingstad, E. D., Zuidema, P. and Chandra, A. S. 2017. Cold Pools and their influence on the tropical marine boundary layer. *J. Atmos. Sci.* **74**, 1149–1168.

Dione, C., Lothon, M., Badiane, D., Campistron, B., Couvreux, F. and co-authors. 2014. Phenomenology of Sahelian convection observed in Niamey during the early monsoon. *Q.J.R. Meteorol. Soc.* **140**, 500–516.

Durran, D. R. 1989. Improving the anelastic approximation. *J. Atmos. Sci.* **46**, 1453–1461.

Durran, D. R. and Klemp, J. B. 1983. A compressible model for the simulation of moist mountain waves. *Mon. Wea. Rev.* **111**, 2341–2361.

Ebert, E. E. and Curry, J. A. 1992. A parameterization of ice cloud optical properties for climate models. *J. Geophys. Res.* **97**, 3831–3836.

Emori, S. and Brown, S. J. 2005. Dynamic and thermodynamic changes in mean and extreme precipitation under changed climate. *Geophys. Res. Lett.* **32**, L17706.

Esau, I. 2014. Indirect air–sea interactions simulated with a coupled turbulence-resolving model. *Ocean Dyn.* **64**, 689–705.

Feng, Z., Hagos, S., Rowe, A. K., Burleyson, C. D., Martini, M. N. and co-authors. 2015. Mechanisms of convective cloud organization by cold pools over tropical warm ocean during the AMIE/DYNAMO field campaign. *J. Adv. Model. Earth Syst.* **7**, 357–381.

Feingold, G., Koren, I., Wang, H. L., Xue, H. W. and Brewer, W. A. 2010. Precipitation-generated oscillations in open cellular cloud fields. *Nature* **466**, 849–852.

Froidevaux, P., Schlemmer, L., Schmidli, J., Langhans, W. and Schär, C. 2014. Influence of the background wind on the local soil moisture–precipitation feedback. *J. Atmos. Sci.* **71**, 782–799.

Fu, Q. 1996. An accurate parameterization of the solar radiative properties of cirrus clouds for climate models. *J. Climate.* **9**, 2058–2082.

Fu, Q., Yang, P. and Sun, W. B. 1998. An accurate parameterization of the infrared radiative properties of cirrus clouds for climate models. *J. Climate* **11**, 2223–2237.

Etling, D. and Brown, R. A. 1993. Roll vortices in the planetary boundary layer: A review. *Bound-Layer Meteorol.* **65**, 215–248.

Gal-Chen, T. and Somerville, R. C. J. 1975. On the use of a coordinate transformation for the solution of the Navier-Stokes equations. *J. Comput. Phys.* **17**, 209–228.

Germano, M., Piomelli, U., Moin, P. and Cabot, W. H. 1991. A dynamic subgrid-scale eddy viscosity model. *Phys. Fluids A* **3**, 1760–1765.

Golaz, J. C., Larson, V. E. and Cotton, W. R. 2002. A PDF-based model for boundary layer clouds. Part I: Method and model description. *J. Atmos. Sci.* **59**, 3540–3551.

Grabowski, W. W., Wu, X. and Moncrieff, M. W. 1996. Cloud-resolving modeling of tropical cloud systems during phase III of GATE. Part I: two-dimensional experiments. *J. Atmos. Sci.* **53**, 3684–3709.

Grabowski, W. W., Wu, X., Moncrieff, M. W. and Hall, W. D. 1998. Cloud-resolving modeling of cloud systems during phase III of GATE. Part II: effects of resolution and the third spatial dimension. *J. Atmos. Sci.* **55**, 3264–3282.

Grabowski, W. W. 2001. Coupling cloud processes with the large-scale dynamics using the cloud-resolving convection parameterization (CRCP). *J. Atmos. Sci.* **58**, 978–997.

Grabowski, W. W. 2003. MJO-like coherent structures: sensitivity simulations using the cloud-resolving convection parameterization (CRCP). *J. Atmos. Sci.* **60**, 847–864.

Grabowski, W. W. 2016. Towards global large eddy simulation: super-parameterization revisited. *J. Meteorol. Soc. Japan.* **94**, 327–344.

Grandpeix, J. Y. and Lafore, J. P. 2010. A density current parameterization coupled with emanuel's convection scheme. Part I: the models. *J. Atmos. Sci.* **67**, 881–897.

Gregory, D. and Miller, M. J. 1989. A numerical study of the parametrization of deep tropical convection. *Q.J.R. Meteorol. Soc.* **115**, 1209–1241.

Gregory, D. 2001. Estimation of entrainment rate in simple models of convective clouds. *Q.J.R. Meteorol. Soc.* **127**, 53–72.

Gregory, D. and Guichard, F. 2002. Aspects of the parametrization of organized convection: contrasting cloud-resolving model and single-column model realizations. *Q.J.R. Meteorol. Soc.* **128**, 625–646.

Griffin, B. M. and Larson, V. E. 2016. Parameterizing microphysical effects on variances and covariances of moisture and heat content using a multivariate probability density function: a study with CLUBB (tag MVCS). *Geosci. Model Dev.* **9**, 4273–4295.

Guichard, F. 1995. *Impact of a cloud ensemble on the large scale environment as obtained with a cloud resolving model (cases GATE and TOGA-COARE).* PhD Thesis. Institut National Polytechnique de Toulouse, Toulouse, France. Thesis No. 1995INPT034H.

Guichard, F., Lafore, J.-P. and Redelsperger, J.-L. 1997. Thermodynamical impact and internal structure of a tropical convective cloud system. *Q.J.R. Meteorol. Soc.* **123**, 2297–2324.

Guichard, F., Redelsperger, J.-L. and Lafore, J.-R. 2000. Cloud-resolving simulation of convective activity during TOGA-COARE: sensitivity to external sources of uncertainties. *Q.J.R. Meteorol. Soc.* **126**, 3067–3095.

Guichard, F., Petch, J. C., Redelsperger, J.-L., Bechtold, P., Chaboureau, J.-P. and co-authors. 2004. Modelling the diurnal cycle of deep precipitating convection over land with cloud-resolving models and single-column models. *Q.J.R. Meteorol. Soc.* **130**, 3139–3172.

Heinze, R., Dipankar, A., Henken, C. C., Moseley, C., Sourdeval, O. and co-authors. 2017. Large-eddy simulations over Germany using ICON: a comprehensive evaluation. *Q.J.R. Meteorol. Soc.* **143**, 69–100.

Held, I. M., Hemler, R. S. and Ramaswamy, V. 1993. Radiative-convective equilibrium with explicit two-dimensional moist convection. *J. Atmos. Sci.* **50**, 3909–3927.

Heus, T., van Dijk, G., Jonker, H. J. J. and van den Akker, H. E. A. 2008. Mixing in shallow cumulus clouds studied by Lagrangian particle tracking. *J. Atmos. Sci.* **65**, 2581–2597.

Heus, T., van Heerwaarden, C. C., Jonker, H. J. J., Pier Siebesma, A., Axelsen, S. and co-authors. 2010. Formulation of the Dutch Atmospheric Large-Eddy Simulation (DALES) and overview of its applications. *Geosci. Model Dev.* **3**, 415–444.

Holloway, C. E., Woolnough, S. J. and Lister, G. M. 2013. The effects of explicit versus parameterized convection on the MJO in a large-domain high-resolution tropical case study. Part I: Characterization of large-scale organization and propagation. *J. Atmos. Sci.* **70**, 1342–1369.

Hong, S.-Y. and Pan, H.-L. 1996. Nonlocal boundary layer vertical diffusion in a medium-range forecast model. *Mon. Wea. Rev.* **124**, 2322–2339.

Honnert, R., Masson, V. and Couvreux, F. 2011. A diagnostic for evaluating the representation of turbulence in atmospheric models at the kilometric scale. *J. Atmos. Sci.* **68**, 3112–3131.

Hourdin, F., Couvreux, F. and Menut, L. 2002. Parameterization of the dry convective boundary layer based on a mass flux representation of thermals. *J. Atmos. Sci.* **59**, 1105–1123.

Hourdin, F., Grandpeix, J.-Y., Rio, C., Bony, S., Jam, A. and co-authors. 2013. LMDZ5B: the atmospheric component of the IPSL climate model with revisited parameterizations for clouds and convection. *Clim. Dyn.* **40**, 2193–2222.

Hourdin, F., Mauritsen, T., Gettelman, A., Golaz, J. C., Balaji, V. and co-authors. 2016. The art and science of climate model tuning. *Bull. Amer. Meteorol. Soc.* **98**, 589–602.

Hourdin, F., Musat, I., Bony, S., Braconnot, P., Codron, F. and co-authors. 2006. The LMDZ4 general circulation model: climate performance and sensitivity to parametrized physics with emphasis on tropical convection. *Clim. Dyn.* **27**, 787–813.

Houze, R. A. Jr, Cheng, C.-P., Leary, C. A. and Gamache, J. F. 1980. Diagnosis of cloud mass and heat fluxes from radar and synoptic data. *J. Atmos. Sci.* **37**, 754–773.

Houze, R. A. Jr and Betts, A. K. 1981. Convection in GATE. *Rev. Geophys.* **19**, 541–576.

Huang, Q., Marsham, J. H., Parker, D. J., Tian, W. and Weckwerth, T. 2009. A comparison of roll and nonroll convection and the subsequent deepening moist convection: an LEM case study based on SCMS data. *Mon. Wea. Rev.* **137**, 350–365.

Jakub, F. and Mayer, B. 2016. 3-D radiative transfer in large-eddy simulations experiences coupling the TenStream solver to the UCLA-LES. *Geosci. Mod. Dev.* **9**, 1413–1422.

Jam, A., Hourdin, F., Rio, C. and Couvreux, F. 2013. Resolved versus parametrized boundary-layer plumes. Part III: Derivation of a statistical scheme for cumulus clouds. *Bound-Layer Meteorol.* **147**, 421–441.

Jonas, P. R. 1990. Observations of cumulus cloud entrainment. *Atmos. Res.* **25**, 105–127.

Jonker, H. J. J., Heus, T. and Sullivan, P. P. 2008. A refined view of vertical mass transport by cumulus convection. *Geophys. Res. Lett.* **35**, L07810.

Keil, C., Heinlein, F. and Craig, G. C. 2014. The convective adjustment time-scale as indicator of predictability of convective precipitation. *Q.J.R. Meteorol. Soc.* **140**, 480–490.

Kendon, E. J., Roberts, N. M., Fowler, H. J., Roberts, M. J., Chan, S. C. and co-authors. 2014. Heavier summer downpours with climate change revealed by weather forecast resolution model. *Nat. Clim. Change* **4**, 570–576.

Kessler, E. 1969. On the distribution and continuity of water substance in atmospheric circulation. *AMS Meteorol. Monogr.* **10**, 1–84. DOI:10.1007/978-1-935704-36-2_1.

Khairoutdinov, M. and Kogan, Y. 2000. A new cloud physics parameterization in a large-eddy simulation model of marine stratocumulus. *Mon. Wea. Rev.* **128**, 229–243.

Khairoutdinov, M. F., Randall, D. A. and DeMott, C. 2005. Simulations of the atmospheric general circulation using a cloud-resolving model as a superparameterization of physical processes. *J. Atmos. Sci.* **62**, 2136–2154.

Khairoutdinov, M. and Randall, D. 2006. High-resolution simulation of shallow-to-deep convection transition over land. *J. Atmos. Sci.* **63**, 3421–3436.

Khairoutdinov, M. F., Krueger, S. K., Moeng, C.-H., Bogenschutz, P. A. and Randall, D. A. 2009. Large-eddy simulation of maritime deep tropical convection. *J. Adv. Model. Earth Syst.* **1**, 15.

Kirshbaum, D. J. and Grant, A. L. M. 2012. Invigoration of cumulus cloud fields by mesoscale ascent. *Q.J.R. Meteorol. Soc.* **138**, 2136–2150.

Klemp, J. B. and Wilhelmson, R. B. 1978. The simulation of three-dimensional convective storm dynamics. *J. Atmos. Sci.* **35**, 1070–1096.

Klemp, J. B. 2011. A terrain-following coordinate with smoothed coordinate surfaces. *Mon. Wea. Rev.* **139**, 2163–2169.

Klinger, C. and Mayer, B. 2016. The neighboring column approximation (NCA) – A fast approach for the calculation of 3D thermal heating rates in cloud resolving models. *J. Quant. Spectrosc. Radiat. Transf.* **168**, 17–28.

Kogan, Y. L., Khairoutdinov, M. P., Lilly, D. K., Kogan, Z. N. and Liu, Q. 1995. Modeling of stratocumulus cloud layers in a large eddy simulation model with explicit microphysics. *J. Atmos. Sci.* **52**, 2923–2940.

Krueger, S. K. 1988. Numerical simulation of tropical cumulus clouds and their interaction with the subcloud layer. *J. Atmos. Sci.* **45**, 2221–2250.

Krueger, S. K., Fu, Q., Liou, K. N. and Chin, H.-N. S. 1995. Improvements of an ice-phase microphysics parameterization for use in numerical simulations of tropical convection. *J. Appl. Meteorol.* **34**, 281–287.

Krueger, S. K., Morrison, H. and Fridlind, A. M. 2016. Cloud-resolving modeling: ARM and the GCSS story. *AMS Meteorol. Monogr.* **57**, 25.1–25.16. DOI:10.1175/AMSMONOGRAPHS-D-15-0047.1.

Kuettner, J. P. 1971. Cloud bands in the earth's atmosphere. *Tellus* **23**, 404–425.

Kurowski, M. J., Grabowski, W. W. and Smolarkiewicz, P. K. 2014. Anelastic and compressible simulation of moist deep convection. *J. Atmos. Sci.* **71**, 3767–3787.

Lafore, J.-P., Redelsperger, J.-L. and Jaubert, G. 1988. Comparison between a 3-dimensional simulation and Doppler Radar data of a tropical squall line – transports of mass, momentum, heat, and moisture. *J. Atmos. Sci.* **45**, 3483–3500.

Lafore, J. P., Stein, J., Asencio, N., Bougeault, P., Ducrocq, V. and co-authors. 1998. The Meso-NH atmospheric simulation system. Part I: adiabatic formulation and control simulations. *Ann. Geophys.* **16**, 90–109.

Larson, V. E., Golaz, J.-C. and Cotton, W. R. 2002. Small-scale and mesoscale variability in cloudy boundary layers: joint probability density functions. *J. Atmos. Sci.* **59**, 3519–3539.

LeMone, M. A. and Pennell, W. T. 1976. The relationship of trade wind cumulus distribution to subcloud layer fluxes and structure. *Mon. Wea. Rev.* **104**, 524–539.

Lenderink, G., Siebesma, A. P., Cheinet, S., Irons, S., Jones, C. G. and co-authors. 2004. The diurnal cycle of shallow cumulus clouds over land: a single-column model intercomparison study. *Q.J.R. Meteorol. Soc.* **130**, 3339–3364.

Lenderink, G. and van Meijgaard, E. 2008. Increase in hourly precipitation extremes beyond expectations from temperature changes. *Nat. Geosci.* **1**, 511–514.

Lilly, D. K. 1962. On the numerical simulation of buoyant convection. *Tellus* **14**, 148–172.

Lilly, D. 1967. *The representation of small-scale turbulence in numerical simulation experiments* Proceedings of the IBM Scientific Computing Symposium on Environmental Science, Yorktown Heights, NY, 195–210.

Lin, C. and Arakawa, A. 1997. The macroscopic entrainment processes of simulated cumulus ensemble. Part I: Entrainment sources. *J. Atmos. Sci.* **54**, 1027–1043.

Lin, Y.-L., Farley, R. D. and Orville, H. D. 1983. Bulk parameterization of the snow field in a cloud model. *J. Climate Appl. Meteorol.* **22**, 1065–1092.

Lin, J. L., Kiladis, G. N., Mapes, B. E., Weickmann, K. M., Sperber, K. R. and co-authors. 2006. Tropical intraseasonal variability in 14 IPCC AR4 climate models. Part I: convective signals. *J. Clim.* **19**, 2665–2690.

Liu, A. Q. G., Moore, W. K., Tsuboki, K. and Renfrew, I. A. 2004. A high-resolution simulation of convective roll clouds during a cold-air outbreak. *Geophys. Res. Lett.* **31**, L03101.

Lohou, F. and Patton, E. 2014. Surface energy balance and buoyancy response to shallow cumulus shading. *J. Atmos. Sci.* **71**, 665–682.

Lothon, M., Couvreux, F., Donier, S., Guichard, F., Lacarrère, P. and co-authors. 2007. Impact of coherent eddies on airborne measurements of vertical turbulent fluxes. *Bound-Layer Meteorol.* **124**, 425–447.

Ludlam, F. H. 1966. Cumulus and cumulonimbus convection. *Tellus* **18**, 687–698.

Malkus, J. S. 1953. Comment on 'Bubble theory of penetrative convection' by Scorer, R. S., Ludlam, F. H. and Stommel, 1953. *Q.J.R. Meteorol. Soc.* **79**, 288–293.

Manabe, S. and Wetherald, R. T. 1967. Thermal equilibrium of the atmosphere with a given distribution of relative humidity. *J. Atmos. Sci.* **24**, 241–259.

Maronga, B., Gryschka, M., Heinze, R., Hoffmann, F., Kanani-Sühring, F. and co-authors. 2015. The Parallelized Large-Eddy Simulation Model (PALM) version 4.0 for atmospheric and oceanic flows: model formulation, recent developments, and future perspectives. *Geosci. Model Dev.* **8**, 2515–2551.

Marshall, J. S. and Palmer, W. Mc K 1948. The distribution of raindrops with size. *J. Meteorol.* **5**, 165–166.

Marsham, J. H., Knippertz, P., Dixon, N. S., Parker, D. J. and Lister, G. 2011. The importance of the representation of deep convection for modeled dust-generating winds over West Africa during summer. *Geophys. Res. Lett.* **38**, L16803.

Marsham, J. H., Dixon, N., Garcia-Carreras, L., Lister, G. M. S., Parker, D. J. and co-authors. 2013. The role of moist convection in the West African monsoon system: Insights from continental-scale convection-permitting simulations. *Geophys. Res. Lett.* **40**, 1843–1849.

Mason, P. J. 1989. Large-eddy simulation of the convective atmospheric boundary layer. *J. Atmos. Sci.* **46**, 1492–1516.

Matheou, G., Chung, D., Nuijens, L., Stevens, B. and Teixeira, J. 2011. On the fidelity of large-eddy simulation of shallow precipitating cumulus convection. *Mon. Wea. Rev.* **139**, 2918–2939.

Mellado, J. P., Stevens, B., Schmidt, H. and Peters, N. 2009. Buoyancy reversal in cloud-top mixing layers. *Q.J.R. Meteorol. Soc.* **135**, 963–978.

Mellor, G. L. 1977. The gaussian cloud model relations. *J. Atmos. Sci.* **34**, 356–358.

Meredith, E. P., Semenov, V. A., Maraun, D., Park, W. and Chernokulsky, A. V. 2015. Crucial role of Black Sea warming in amplifying the 2012 Krymsk precipitation extreme. *Nat. Geosci.* **8**, 615–619.

Mesinger, F. and Arakawa, A. 1976. Numerical methods used in atmospheric models. *GARP Publications Series No. 17*. WMO/ICSU Joint Organizing Committee, 64 pp.

Meyers, M. P., Walko, R. L., Harrington, J. Y. and Cotton, W. R. 1997. New RAMS cloud microphysics parameterization. Part II: The two-moment scheme. *Atmos. Res.* **45**, 3–39.

Milbrandt, J. A. and Yau, M. K. 2005. A multimoment bulk microphysics parameterization. Part I: Analysis of the role of the spectral shape parameter. *J. Atmos. Sci.* **62**, 3051–3064.

Miller, M. J. and Pearce, R. P. 1974. A three dimensional primitive equation model of cumulonimbus convection. *Q.J.R. Meteorol. Soc.* **100**, 133–154.

Misra, A. and Pullin, D. I. 1997. A vortex-based subgrid stress model for large-eddy simulation. *Phys. Fluids.* **9**, 2443–2454.

Miura, H., Satoh, M., Nasuno, T., Noda, A. T. and Oouchi, K. 2007. A Madden-Julian oscillation event realistically simulated by a global cloud-resolving model. *Science* **318**, 1763–1765.

Miyakawa, T., Satoh, M., Miura, H., Tomita, H., Yashiro, H. and co-authors. 2014. Madden-Julian oscillation prediction skill of a new-generation global model demonstrated using a supercomputer. *Nat. Commun.* **5**, 3769.

Moeng, C. 1984. A large-eddy-simulation model for the study of planetary boundary-layer turbulence. *J. Atmos. Sci.* **41**, 2052–2062.

Moeng, C.-H. and Sullivan, P. P. 2002. Large-eddy simulation. In: Encyclopedia of Atmospheric Sciences. 2nd ed (eds. J. R. Holton, J. Pyle and F. Zhang) Vol. 4. Academic Press, San Diego, CA, pp. 243–240.

Morrison, H. and Grabowski, W. W. 2008. A novel approach for representing ice microphysics in models: description and tests using a kinematic framework. *J. Atmos. Sci.* **65**, 1528–1548.

Morrison, H., Thompson, G. and Tatarskii, V. 2009. Impact of cloud microphysics on the development of trailing stratiform precipitation in a simulated squall line: comparison of one- and two-moment schemes. *Mon. Wea. Rev.* **137**, 991–1007.

Muller, C. J., O'Gorman, P. A. and Back, L. E. 2011. Intensification of precipitation extremes with warming in a cloud-resolving model. *J. Climate* **24**, 2784–2800.

Muller, C. J. 2013. Impact of convective organization on the response of tropical precipitation extremes to warming. *J Climate* **26**, 5028–5043.

Müller, G. and Chlond, A. 1996. Three-dimensional numerical study of cell broadening during cold-air outbreaks. *Bound-Layer Meteorol.* **81**, 289–323.

Neggers, R. A. J., Jonker, H. J. J. and Siebesma, A. P. 2003a. Size statistics of cumulus cloud populations in large-eddy simulations. *J Atmos Sci.* **60**, 1060–1074.

Neggers, R. A. J., Duynkerke, P. G. and Rodts, S. M. A. 2003b. Shallow cumulus convection: a validation of large-eddy simulation against aircraft and Landsat observations. *Quart. J. Roy. Met. Soc.* **129**, 2671–2696.

Neggers, R. A. J. 2009. A dual mass flux framework for boundary layer convection. Part II: clouds. *J. Atmos. Sci.* **66**, 1489–1506.

Neggers, R. A. J. 2015. Attributing the behavior of low-level clouds in large-scale models to subgrid-scale parameterizations. *J. Adv. Model. Earth Syst.* **7**, 2029–2043.

O'Gorman, P. A. 2015. Precipitation extremes under climate change. *Curr. Clim. Change Rep.* **1**, 49–59.

Ogura, Y. and Phillips, N. A. 1962. Scale analysis of deep and shallow convection in the atmosphere. *J. Atmos. Sci.* **19**, 173–179.

Ogura, Y. 1963. The evolution of a moist convective element in a shallow, conditionally unstable atmosphere: a numerical calculation. *J. Atmos. Sci.* **20**, 407–424.

Orszag, S. 1971. Numerical simulation of incompressible flows within simple boundaries: accuracy. *J. Fluid Mech.* **49**, 75–112.

Oue, M., Kollias, P., North, K. W., Tatarevic, A., Endo, S. and co-authors. 2016. Estimation of cloud fraction profile in shallow convection using a scanning cloud radar. *Geophys. Res. Lett.* **43**, 10998–11006.

Oueslati, B. and Bellon, G. 2013. Convective entrainment and large-scale organization of tropical precipitation: sensitivity of the CNRM-CM5 hierarchy of models. *J. Climate* **26**, 2931–2946.

Panthou, G., Vischel, T. and Lebel, T. 2014. Recent trends in the regime of extreme rainfall in the Central Sahel. *Int. J. Climatol.* **34**, 3998–4006.

Park, S., Heus, T. and Gentine, P. 2017. Role of convective mixing and evaporative cooling in shallow convection. *J. Geophys. Res* **122**, 5351–5363.

Patton, E. G., Sullivan, P. P. and Moeng, C. H. 2005. The influence of idealized heterogeneity on wet and dry planetary boundary layers coupled to the land surface. *J. Atmos. Sci.* **62**, 2078–2097.

Pergaud, J., Masson, V., Malardel, S. and Couvreux, F. 2009. A parameterization of dry thermals and shallow cumuli for mesoscale numerical weather prediction. *Bound-Layer Meteorol.* **132**, 83–106.

Phillips, V. T., Donner, L. J. and Garner, S. T. 2007. Nucleation processes in deep convection simulated by a cloud-system-resolving model with double-moment bulk microphysics. *J. Atmos. Sci.* **64**, 738–761.

Pielke, R. A. Sr. 2013. *Mesoscale Meteorological Modeling.* 3rd ed., Vol. 98, International Geophysics Series, Academic press, San Diego, CA.

Pincus, R. 2013. Radiation across spatial scales (and model resolutions). *Proceedings of the ECMWF Workshop on Parametrization of Clouds and Precipitation Across Model Resolutions*, Reading, UK, pp. 109–115.

Pincus, R. and Stevens, B. 2009. Monte Carlo spectral integration: a consistent approximation for radiative transfer in large eddy simulations. *J. Adv. Model. Earth Syst.* **1**, 1–9.

Pope, S. B. 2000. *Turbulent Flows* Cambridge University Press, Cambridge.

Prein, A. F., Langhans, W., Fosser, G., Ferrone, A., Ban, N. and co-authors. 2015. A review on regional convection-permitting climate modeling: Demonstrations, prospects, and challenges. *Rev. Geophys.* **53**, 323–361.

Raasch, S. and Schröter, M. 2001. PALM – A large-eddy simulation model performing on massively parallel computers. *Meteorol. Z.* **10**, 363–372.

Randall, D. A., Xu, K.-M., Somerville, R. J. C. and Iacobellis, S. 1996. Single-column models and cloud ensemble models as links between observations and climate models. *J. Climate* **9**, 1683–1697.

Randall, D. A., Khairoutdinov, M., Arakawa, A. and Grabowski, W. 2003. Breaking the cloud parameterization deadlock. *Bull. Amer. Meteorol. Soc.* **84**, 1547–1564.

Raymond, D. J. and Zeng, X. 2005. Modelling tropical atmospheric convection in the context of the weak temperature gradient approximation. *Q.J.R. Meteorol. Soc.* **131**, 1301–1320.

Redelsperger, J.-L. and Sommeria, G. 1981. Methode de representation de la turbulence d'echelle inferieure a la maille pour un modele tri-dimensionnel de convection nuageuse. *Bound-Layer Meteorol.* **21**, 509–530.

Redelsperger, J.-L. and Sommeria, G. 1986. Three-Dimensional Simulation of a Convective Storm: Sensitivity Studies on Subgrid Parameterization and Spatial Resolution. *J. Atmos. Sci.* **43**, 2619–2635.

Redelsperger, J.-L. and Lafore, J.-P. 1988. A Three-Dimensional Simulation of a Tropical Squall Line: Convective Organization and Thermodynamic Vertical Transport. *J. Atmos. Sci.* **45**, 1334–1356.

Redelsperger, J. L., Brown, P. R. A., Guichard, F., How, C., Kawasima, M. and co-authors. 2000a. A gcss model intercomparison for a tropical squall line observed during toga-coare. I: Cloud-resolving models. *Q.J.R. Meteorol. Soc.* **126**, 823–863.

Redelsperger, J.-L., Guichard, F. and Mondon, S. 2000b. A Parameterization of Mesoscale Enhancement of Surface Fluxes for Large-Scale Models. *J. Climate.* **13**, 402–421.

Redelsperger, J., Parsons, D. B. and Guichard, F. 2002. Recovery Processes and Factors Limiting Cloud-Top Height following the Arrival of a Dry Intrusion Observed during TOGA COARE. *J. Atmos. Sci.* **59**, 2438–2457.

Ricard, D., Lac, C., Riette, S., Legrand, R. and Mary, A. 2013. Kinetic energy spectra characteristics of two convection-permitting limited-area models AROME and Meso-NH. *Q.J.R. Meteorol. Soc.* **139**, 1327–1341.

Rio, C. and Hourdin, F. 2008. A Thermal Plume Model for the Convective Boundary Layer: Representation of Cumulus Clouds. *J. Atmos. Sci.* **65**, 407–425.

Rio, C., Hourdin, F., Couvreux, F. and Jam, A. 2010. Resolved versus Parametrized Boundary-Layer Plumes. Part II: Continuous Formulations of Mixing Rates for Mass-Flux Schemes. *Bound-Layer Meteorol.* **135**, 469–483.

Robe, F. R. and Emanuel, K. A. 1996. Moist Convective Scaling: Some Inferences from Three-Dimensional Cloud Ensemble Simulations. *J. Atmos. Sci.* **53**, 3265–3275.

Rochetin, N., Couvreux, F., Grandpeix, J.-Y. and Rio, C. 2014. Deep Convection Triggering by Boundary Layer Thermals. Part I: LES Analysis and Stochastic Triggering Formulation. *J. Atmos. Sci.* **71**, 496–514.

Rochetin, N., Couvreux, F. and Guichard, F. 2017. Morphology of breeze circulations induced by surface flux heterogeneities and their impact on convection initiation. *Q.J.R. Meteorol. Soc.* **143**, 463–478.

Romps, D. M. 2008. The Dry-Entropy Budget of a Moist Atmosphere. *J. Atmos. Sci.* **65**, 3779–3799.

Romps, D. M. 2010. A Direct Measure of Entrainment. *J. Atmos. Sci.* **67**, 1908–1927.

Romps, D. M. and Kuang, Z. 2010. Nature versus Nurture in Shallow Convection. *J. Atmos. Sci.* **67**, 1655–1666.

Romps, D. M. 2011. Response of Tropical Precipitation to Global Warming. *J. Atmos. Sci.* **68**, 123–138.

Ruppert, J. H. 2016. Diurnal timescale feedbacks in the tropical cumulus regime. *J. Adv. Model. Earth Syst.* **8**, 1483–1500.

Sagaut, P. 2006. *Large-eddy simulation for incompressible flows – An introduction*, 3rd ed. Springer-Verlag, Scientific Computation series, 556 pages.

Sanderson, B. M., Piani, C., Ingram, W. J., Stone, D. A. and Allen, M. R. 2008. Towards constraining climate sensitivity by linear analysis of feedback patterns in thousands of perturbed-physics GCM simulations. *Clim. Dyn.* **30**, 175–190.

Sandu, I. and Stevens, B. 2011. On the Factors Modulating the Stratocumulus to Cumulus Transitions. *J. Atmos. Sci.* **68**, 1865–1881.

Satoh, M., Matsuno, T., Tomita, H., Miura, H., Nasuno, T. and co-authors. 2008. Nonhydrostatic icosahedral atmospheric model (NICAM) for global cloud resolving simulations. *J. Comput. Phys.* **227**, 3486–3514.

Savic-Jovcic, V. and Stevens, B. 2008. The Structure and Mesoscale Organization of Precipitating Stratocumulus. *J. Atmos. Sci.* **65**, 1587–1605.

Schalkwijk, J., Jonker, H. J. J., Siebesma, A. P. and Bosveld, F. C. 2015. A Year-Long Large-Eddy Simulation of the Weather over Cabauw: An Overview. *Mon. Wea. Rev.* **143**, 828–844.

Schär, C., Leuenberger, D., Fuhrer, O., Lüthi, D. and Girard, C. 2002. A new terrain-following vertical coordinate formulation for atmospheric prediction models. *Mon. Wea. Rev.* **130**, 2459–2480.

Schlemmer, L., Hohenegger, C., Schmidli, J., Bretherton, C. S. and Schär, C. 2011. An Idealized Cloud-Resolving Framework for the Study of Midlatitude Diurnal Convection over Land. *J. Atmos. Sci.* **68**, 1041–1057.

Schlemmer, L. and Hohenegger, C. 2014. The Formation of Wider and Deeper Clouds as a Result of Cold-Pool Dynamics. *J. Atmos. Sci.* **71**, 2842–2858.

Schmidt, H. and Schumann, U. 1989. Coherent structure of the convective boundary layer derived from large-eddy simulations. *J. Fluid Mech.* **200**, 511–562.

Schröter, M., Raasch, S. and Jansen, H. 2005. Cell broadening revisited: Results from high-resolution large-eddy simulations of cold air outbreaks. *J. Atmos. Sci.* **62**, 2023–2032.

Schumann, U. and Sweet, R. 1988. Fast Fourier transforms for direct solution of poisson's equation with staggered boundary conditions. *J. Comput. Phys.* **75**, 123–137.

Seifert, A. and Beheng, K. D. 2006. A two-moment cloud microphysics parameterization for mixed-phase clouds. Part 1: Model description. *Meteorol. Atmos. Phys.* **92**, 45–66.

Seifert, A. and Heus, T. 2013. Large-eddy simulation of organized precipitating trade wind cumulus clouds. *Atmos. Chem. Phys.* **13**, 5631–5645.

Sessions, S. L., Sugaya, S., Raymond, D. J. and Sobel, A. H. 2010. Multiple equilibria in a cloud-resolving model using the weak temperature gradient approximation. *J. Geophys. Res.* **115**, D12110.

Seity, Y., Brousseau, P., Malardel, S., Hello, G., Bénard, P., Bouttier, F. and co-authors. 2011. The AROME-France convective-scale operational model. *Mon. Wea. Rev.* **139**, 976–991.

Siebesma, A. P. and Holtslag, A. A. M. 1996. Model impacts of entrainment and detrainment rates in shallow cumulus convection. *J. Atmos. Sci.* **53**, 2354–2364.

Siebesma, A. P., Bretherton, C. S., Brown, A., Chlond, A., Cuxart, J. and co-authors. 2003. A large eddy simulation intercomparison study of shallow cumulus convection. *J. Atmos. Sci.* **60**, 1201–1219.

Siebesma, A. P., Soares, P. M. M. and Teixeira, J. 2007. A combined eddy-diffusivity mass-flux approach for the convective boundary layer. *J. Atmos. Sci.* **64**, 1230–1248.

Simpson, J. and Wiggert, V. 1969. Models of precipitating cumulus towers. *Mon. Wea. Rev.* **97**, 471–489.

Singh, M. S. and O'Gorman, P. A. 2014. Influence of microphysics on the scaling of precipitation extremes with temperature. *Geophys. Res. Lett.* **41**, 6037–6044.

Singleton, A. and Toumi, R. 2013. Super-Clausius–Clapeyron scaling of rainfall in a model squall line. *Q.J.R Meteorol. Soc.* **139**, 334–339.

Skamarock, W. C., Klemp, J. B., Duda, M. G., Fowler, L. D., Park, S. H. and co-authors. 2012. A multiscale nonhydrostatic atmospheric model using centroidal voronoi tesselations and C-grid staggering. *Mon. Wea. Rev.* **140**, 3090–3105.

Slingo, A. 1989. A GCM parameterization for the shortwave radiative properties of water clouds. *J. Atmos. Sci.* **46**, 1419–1427.

Smagorinsky, J. 1963. General circulation experiments with the primitive equations. I. The basic experiment. *Mon. Wea. Rev.* **91**, 99–164.

Smolarkiewicz, P. K. and Grabowski, W. W. 1990. The multidimensional positive definite advection transport algorithm: nonoscillatory option. *J. Comput. Phys.* **86**, 355–375.

Sobel, A. H. and Bretherton, C. S. 2000. Modeling tropical precipitation in a single column. *J. Climate* **13**, 4378–4392.

Sommeria, G. 1976. Three-dimensional simulation of turbulent processes in an undisturbed trade wind boundary layer. *J. Atmos. Sci.* **33**, 216–241.

Sommeria, G. and Deardorff, J. W. 1977. Subgrid-scale condensation in models of nonprecipitating clouds. *J. Atmos. Sci.* **34**, 344–355.

Sommeria, G. and LeMone, M. A. 1978. Direct testing of a three-dimensional model of the planetary boundary layer against experimental data. *J. Atmos. Sci.* **35**, 25–39.

Stephens, G. 1978. Radiation profiles in extended water clouds. II: Parameterization schemes. *J. Atmos. Sci.* **35**, 2123–2132.

Stevens, B., Ackerman, A. S., Albrecht, B. A., Brown, A. R., Chlond, A. and co-authors. 2001. Simulations of trade wind cumuli under a strong inversion. *J. Atmos. Sci.* **58**, 1870–1891.

Stevens, B. and Lenschow, D. H. 2001. Observations, experiments, and large eddy simulation. *Bull. Amer. Meteorol. Soc.* **82**, 283–294.

Stevens, B., Moeng, C.-H. and Sullivan, P. P. 1999. Large-eddy simulations of radiatively driven convection: sensitivities to the representation of small scales. *J. Atmos. Sci.* **56**, 3963–3984.

Stevens, B., Moeng, C.-H., Ackerman, A. S., Bretherton, C. S., Chlond, A. and co-authors. 2005. Evaluation of large-eddy simulations via observations of nocturnal marine stratocumulus. *Mon. Wea. Rev.* **133**, 1443–1462.

Stevens, B. and Seifert, A. 2008. Understanding macrophysical outcomes of microphysical choices in simulations of shallow cumulus convection. *J. Meteorol. Soc. Japan* **86A**, 143–162.

Sui, C. H., Lau, K. M., Tao, W. K. and Simpson, J. 1994. The tropical water and energy cycles in a cumulus ensemble model. Part I: equilibrium climate. *J. Atmos. Sci.* **51**, 711–728.

Sullivan, P. P., McWilliams, J. C. and Patton, E. G. 2014. Large-eddy simulation of marine atmospheric boundary layers above a spectrum of moving waves. *J. Atmos. Sci.* **71**, 4001–4027.

Sullivan, P. P. and Patton, E. G. 2011. The effect of mesh resolution on convective boundary layer statistics and structures generated by large-eddy simulation. *J. Atmos. Sci.* **68**, 2395–2415.

Sun, Z. and Shine, K. P. 1995. Parameterization of ice cloud radiative properties and its application to the potential climatic importance of mixed-phase clouds. *J. Climate* **8**, 1874–1888.

Takemi, T. and Rotunno, R. 2003. The effects of subgrid model mixing and numerical filtering in simulations of mesoscale cloud systems. *Mon. Wea. Rev.* **131**, 2085–2101.

Takemi, T. and Rotunno, R. 2005. *Corrigendum Mon. Wea. Rev.* **133**, 339–341.

Takemi, T. 2005. Explicit simulations of convective-scale transport of mineral dust in severe convective weather. *J. Meteorol. Soc. Japan.* **83A**, 187–203.

Tao, W.-K. and Soong, S.-T. 1986. A study of the response of deep tropical clouds to mesoscale processes: three-dimensional numerical experiments. *J. Atmos. Sci.* **43**, 2653–2676.

Tao, W. K., Simpson, J. and McCumber, M. 1989. An ice-water saturation adjustment. *Mon. Wea. Rev.* **117**, 231–235.

Tao, W.-K., Simpson, J., Sui, C.-H., Shie, C.-L., Zhou, B. and co-authors. 1999. Equilibrium states simulated by cloud-resolving models. *J. Atmos. Sci.* **56**, 3128–3139.

Taylor, C. M., Belušić, D., Guichard, F., Parker, D. J., Vischel, T. and co-authors. 2017. Frequency of extreme Sahelian storms tripled since 1982 in satellite observations. *Nature* **544**, 475–478.

Thayer-Calder, K. and Randall, D. A. 2009. The role of convective moistening in the Madden–Julian oscillation. *J. Atmos. Sci.* **66**, 3297–3312.

Tiedtke, M. 1989. A comprehensive mass flux scheme for cumulus parameterization in large-scale models. *Mon. Wea. Rev.* **117**, 1779–1800.

Tomita, H., Miura, H., Iga, S., Nasuno, T. and Satoh, M. 2005. A global cloud-resolving simulation: Preliminary results from an aqua planet experiment. *Geophys. Res. Lett.* **32**(8), L08805.

Tompkins, A. M. and Craig, G. C. 1998. Radiative-convective equilibrium in a three-dimensional cloud ensemble model. *Q.J.R. Meteorol. Soc.* **124**, 2073–2097.

Tompkins, A. M. 2000. The impact of dimensionality on long-term cloud-resolving model simulations. *Mon. Wea. Rev.* **128**, 1521–1535.

Tompkins, A. M. 2001. Organization of tropical convection in low vertical wind shears: the role of cold pools. *J. Atmos. Sci.* **58**, 1650–1672.

Tompkins, A. M. and Semie, A. G. 2017. Organization of tropical convection in low vertical wind shears: role of updraft entrainment. *J. Adv. Model. Earth Syst.* **9**, 1046–1068.

Torri, G., Kuang, Z. and Tian, Y. 2015. Mechanisms for convection triggering by cold pools. *Geophys. Res. Lett.* **42**, 1943–1950.

Trapp, R. J. 2013. *Mesoscale-Convective Processes in the Atmosphere*. Cambridge University Press, New York, NY.

Trier, S. B., Chen, F. and Manning, K. W. 2004. A study of convection initiation in a mesoscale model using high-resolution land surface initial conditions. *Mon. Wea. Rev.* **132**, 2954–2976.

Troen, I. W. and Mahrt, L. 1986. A simple model of the atmospheric boundary layer; sensitivity to surface evaporation. *Bound-Layer Meteorol.* **37**, 129–148.

Ulbrich, C. W. 1983. Natural variations in the analytical form of the raindrop size distribution. *J. Climate Appl. Meteorol.* **22**, 1764–1775.

van Zanten, M. C., Stevens, B., Nuijens, L., Siebesma, A. P., Ackerman, A. S. and co-authors. 2011. Controls on precipitation and cloudiness in simulations of trade-wind cumulus as observed during RICO. *J. Adv. Model. Earth Syst.* **3**, M06001.

Vial, J., Dufresne, J. L. and Bony, S. 2013. On the interpretation of inter-model spread in CMIP5 climate sensitivity estimates. *Clim. Dyn.* **41**, 3339–3362.

Vinkovic, I., Aguirre, C., Ayrault, M. and Simoëns, S. 2006. Large-eddy simulation of the dispersion of solid particles in a turbulent boundary layer. *Bound-Layer Meteorol.* **121**, 283–311.

Vogel, R., Nuijens, L. and Stevens, B. 2016. The role of precipitation and spatial organization in the response of trade-wind clouds to warming. *J. Adv. Model. Earth Syst.* **8**, 843–862.

Wang, H. and Feingold, G. 2009. Modeling mesoscale cellular structures and drizzle in marine stratocumulus. Part I: impact of drizzle on the formation and evolution of open cells. *J. Atmos. Sci.* **66**, 3237–3256.

Wang, Y., Zhang, G. J. and Craig, G. C. 2016. Stochastic convective parameterization improving the simulation of tropical precipitation variability in the NCAR CAM5. *Geophys. Res. Lett.* **43**, 6612–6619.

Wapler, K. and Mayer, B. 2008. A fast three-dimensional approximation for the calculation of surface irradiance in large-eddy simulation models. *J. Appl. Meteorol. Climatol.* **47**, 3061–3071.

Warner, J. 1970. On steady-state one-dimensional models of cumulus convection. *J. Atmos. Sci.* **27**, 1035–1040.

Warner, T. T. 2010. *Numerical weather and climate prediction*. Cambridge University Press, Cambridge.

Weckwerth, T. M., Wilson, J. W. and Wakimoto, R. M. 1996. Thermodynamic variability within the convective boundary layer due to horizontal convective rolls. *Mon. Wea. Rev.* **124**, 769–784.

Weckwerth, T. M., Horst, T. W. and Wilson, J. W. 1999. An observational study of the evolution of horizontal convective rolls. *Mon. Wea. Rev.* **127**, 2160–2179.

Weisman, M. L., Skamarock, W. C. and Klemp, J. B. 1997. The resolution dependence of explicitly modeled convective systems. *Mon. Wea. Rev.* **125**, 527–548.

Westra, S., Fowler, H. J., Evans, J. P., Alexander, L. V. and Berg, P. and co-authors. 2014. Future changes to the intensity and frequency of short-duration extreme rainfall. *Rev. Geophys.* **52**, 522–555.

Wicker, L. J. and Skamarock, W. C. 2002. Time-splitting methods for elastic models using forward time schemes. *Mon. Wea. Rev.* **130**, 2088–2097.

Wilhelmson, R. B. and Klemp, J. B. 1981. A three-dimensional numerical simulation of splitting severe storms on 3 April 1964. *J. Atmos. Sci.* **38**, 1581–1600.

Wyngaard, J. C. 2004. Changing the face of small-scale meteorology. In: *Atmospheric Turbulence and Mesoscale Meteorology*. (eds. E. Fedorovich, R. Rotunno and B. Stevens). Cambridge University Press, Cambridge, pp. 17–34.

Wyngaard, J. C. 2010. *Turbulence in the Atmosphere* Cambridge University Press, Cambridge.

Wood, R. 2012. Stratocumulus clouds. *Mon. Wea. Rev.* **140**, 2373–2423.

Wood, R. and Hartmann, D. L. 2006. Spatial variability of liquid water path in marine low cloud: the importance of mesoscale cellular convection. *J. Climate.* **19**, 1748–1764.

Wu, X., Grabowski, W. W. and Moncrieff, M. W. 1998. Long-term behavior of cloud systems in TOGA COARE and their interactions with radiative and surface processes. Part I: two-dimensional modeling study. *J. Atmos. Sci.* **55**, 2693–2714.

Wyant, M. C., Bretherton, C. S., Rand, H. A. and Stevens, D. E. 1997. Numerical simulations and a conceptual model of the stratocumulus to trade cumulus transition. *J. Atmos. Sci.* **54**, 168–192.

Xu, K. M., Arakawa, A. and Krueger, S. K. 1992. The macroscopic behavior of cumulus ensembles simulated by a cumulus ensemble model. *J. Atmos. Sci.* **49**, 2402–2420.

Xu, K. 1994. A statistical analysis of the dependency of closure assumptions in cumulus parameterization on the horizontal resolution. *J. Atmos. Sci.* **51**, 3674–3691.

Xu, K. M. 1995. Partitioning mass, heat, and moisture budgets of explicitly simulated cumulus ensembles into convective and stratiform components. *J. Atmos. Sci.* **52**, 551–573.

Xu, K. M. and Randall, D. A. 1996. Explicit simulation of cumulus ensembles with the GATE Phase III data: comparison with observations. *J. Atmos. Sci.* **53**, 3710–3736.

Xu, K. M. and Randall, D. A. 1999. A sensitivity study of radiative–convective equilibrium in the tropics with a convection-resolving model. *J. Atmos. Sci.* **56**, 3385–3400.

Xu, K.-M., Cederwall, R. T., Donner, L. J., Grabowski, W. W., Guichard, F. and co-authors. 2002. An intercomparison of cloud-resolving models with the ARM summer 1997 IOP data. *Q.J.R. Meteorol. Soc.* **128**, 593–624.

Xue, H., Feingold, G. and Stevens, B. 2008. Aerosol effects on clouds, precipitation, and the organization of shallow cumulus convection. *J. Atmos. Sci.* **65**, 392–406.

Yano, J. I., Guichard, F., Lafore, J. P., Redelsperger, J. L. and Bechtold, P. 2004. Estimations of mass fluxes for cumulus parameterizations from high-resolution spatial data. *J. Atmos. Sci.* **61**, 829–842.

Yano, J.-I., Bister, M., Fuchs, Ž., Gerard, L., Phillips, V. T. and co-authors. 2013. Phenomenology of convection-parameterization closure. *Atmos. Chem. Phys.* **13**, 4111–4131.

Yau, M. K. 1979. Perturbation pressure and cumulus convection. *J. Atmos. Sci.* **36**, 690–694.

Yeo, K. and Romps, D. M. 2013. Measurement of convective entrainment using lagrangian particles. *J. Atmos. Sci.* **70**, 266–277.

Zhang, C. 2005. Madden-Julian oscillation. *Rev. Geophys.* **43**, RG2003.

Zhang, M., Bretherton, C. S., Blossey, P. N., Austin, P. H. and Bacmeister, J. T. 2013. CGILS: Results from the first phase of an international project to understand the physical mechanisms of low cloud feedbacks in single column models. *J. Adv. Model. Earth Syst.* **5**, 826–842.

Zhao, M. and Austin, P. H. 2005. Life cycle of numerically simulated shallow cumulus clouds. Part II: mixing dynamics. *J. Atmos. Sci.* **62**, 1291–1310.

Zhu, P., Albrecht, B. A., Ghate, V. P. and Zhu, Z. 2010. Multiple-scale simulations of stratocumulus clouds. *J. Geophys. Res.* **115**, D23201.

Zuidema, P., Li, Z., Hill, R. J., Bariteau, L., Rilling, B. and co-authors. 2012. On trade wind cumulus cold pools. *J. Atmos. Sci.* **69**, 258–280.